

Over Half of the Negative Crop Yield Variability Explained by Anthropogenic Indicators

Pekka Kinnunen¹, Matias Heino¹, Vilma Sandström¹, Maija Taka¹, Deepak K Ray², and Matti Kummu¹

¹Aalto University

²University of Minnesota

November 21, 2022

Abstract

High crop yield variation between years, impacted for example by extreme weather shocks and by other shocks on the food production system, can have substantial effect on food production. This, in turn introduces vulnerabilities within global food system. To mitigate the effects of these shocks there is a clear need for understanding how different adaptive capacity measures link to the crop yield variability. While existing literature provides many local scale studies on this linkage, no comprehensive global assessment yet exists. We assessed reported crop yield variation for wheat, maize, soybean and rice for time period 1981-2009 by measuring both yield loss risk (variation in negative yield anomalies considering all years) and changes in yields during only dry shock and hot shock years. We used machine learning algorithm XGBoost to assess globally the explanatory power of selected gridded anthropogenic indicators (i.e., adaptive capacity measures; such as Human Development Index, irrigation infrastructure, fertilizer use) on yield variation on 0.5 degree resolution, within climatically similar regions to rule out the role of average climate conditions. We found that the anthropogenic indicators explained 40-60% of yield loss risk variation whereas the indicators provided noticeably lower (5-20%) explanatory power during shock years. On continental scale, especially in Europe and Africa the indicators explained high proportion of the yield loss risk variation (up to around 80%). Assessing crop production vulnerabilities on global scale provides supporting knowledge to target specific adaptation measures, thus contributing to global food security.

1
2
3
4
5
6
7
8
9
10
11
12
13
14

Over Half of the Negative Crop Yield Variability Explained by Anthropogenic Indicators

P. Kinnunen*¹, M. Heino¹, V. Sandström¹, M. Taka¹, D. K. Ray², M. Kummu*¹

¹ Water and Development Research Group, Aalto University, Espoo, Finland

² Institute on the Environment, University of Minnesota, Twin Cities, USA

*Corresponding authors: Pekka Kinnunen (pekka.kinnunen@aalto.fi), Matti Kummu (matti.kummu@aalto.fi)

Key Points:

- Anthropogenic indicators can explain up to 60% of variation for the negative crop yields
- Less than 20 % of variation of crop yield anomalies during temperature or soil moisture shocks can be explained by anthropogenic indicators

15 **Abstract**

16 High crop yield variation between years, impacted for example by extreme weather shocks and by other shocks on the
17 food production system, can have substantial effect on food production. This, in turn introduces vulnerabilities within
18 global food system. To mitigate the effects of these shocks there is a clear need for understanding how different
19 adaptive capacity measures link to the crop yield variability. While existing literature provides many local scale studies
20 on this linkage, no comprehensive global assessment yet exists. We assessed reported crop yield variation for wheat,
21 maize, soybean and rice for time period 1981-2009 by measuring both yield loss risk (variation in negative yield
22 anomalies considering all years) and changes in yields during only dry shock and hot shock years. We used machine
23 learning algorithm XGBoost to assess globally the explanatory power of selected gridded anthropogenic indicators
24 (i.e., adaptive capacity measures; such as Human Development Index, irrigation infrastructure, fertilizer use) on yield
25 variation on 0.5 degree resolution, within climatically similar regions to rule out the role of average climate conditions.
26 We found that the anthropogenic indicators explained 40-60% of yield loss risk variation whereas the indicators
27 provided noticeably lower (5-20%) explanatory power during shock years. On continental scale, especially in Europe
28 and Africa the indicators explained high proportion of the yield loss risk variation (up to around 80%). Assessing crop
29 production vulnerabilities on global scale provides supporting knowledge to target specific adaptation measures, thus
30 contributing to global food security.

31

32 **1 Introduction**

33 The recent developments of population growth, urbanization, economic development, and climate change continue to
34 cause significant pressure on the global food system (FAO, 2019). Food systems are vulnerable to systemic and
35 environmental disruptions which can stem from anthropogenic factors such as shocks in food trade systems or
36 environmental conditions such as unfavorable weather conditions (Cottrell et al., 2019). Short term supply shocks
37 such as abrupt drop in the production quantities or crop yields can result in food scarcity which has propagating effects
38 through global markets (Distefano et al., 2018). On longer term, especially small holders who produce around a third
39 of global food (Ricciardi et al., 2018) face myriad of systemic factors hindering adaptation options, e.g., limited
40 economic and financial resources, lower socioeconomic and educational status or unavailability of appropriate
41 technologies (Cohn et al., 2017). Thus, to increase resilience within food production systems, it is important to identify
42 areas most vulnerable to different disruptions.

43

44 The key drivers of food production shocks are extreme weather events together with geopolitical and economic events
45 (Cottrell et al., 2019). However, the importance of these drivers is characterized by regional variation; for example,
46 food production in South Asia suffers mostly from hydrological extremes (e.g., droughts and floods), whereas
47 geopolitical and economic crises are the main shock drivers in Sub-Saharan Africa (Cottrell et al., 2019). All these
48 shocks impact food security and especially the most vulnerable communities through food availability (Cottrell et al.,
49 2019), food prices (Chatzopoulos et al., 2020) and quality of food (Fahad et al., 2017). To ensure better mitigation to

50 the shocks, and thus more resilient food systems, it is important to better understand the key factors and the
51 geographical features influencing the responses to these shocks.

52

53 Climatic conditions have been shown to be key factors in crop yield variation, explaining approximately 20-60% of
54 the global crop yield variation (Ray et al., 2015; Vogel et al., 2019). However, we lack comprehensive understanding
55 of the other key factors and the potential of human actions to mitigate crop yield losses. Findings from existing studies
56 indicate that anthropogenic indicators related to socio-economic level and food production factors have potential to
57 explain part of this gap. These studies have been focusing especially on droughts and climate change adaptation,
58 suggesting that from vulnerability and adaptive capacity perspective, indicators such as high level of economic activity
59 measured as gross domestic product (Simelton et al., 2009, 2012), human capital (e.g. (Antwi-Agyei et al., 2012;
60 Gbetibouo et al., 2010) or increased irrigation (Fuss et al., 2015; Müller et al., 2018; Troy et al., 2015) seems to
61 correlate well with lower vulnerability or less volatile crop yields. For fertilizer use, key crop production factor, the
62 studied effects have been mixed. Using national scale data Simelton *et al.* (2012) and Kamali *et al.* (2019) found that
63 fertilizer use was linked with lower vulnerability to droughts. On the other hand, Müller *et al.*, (2018) found in a global
64 grid scale modelling study that while higher fertilizer use may lead to lower relative yield variability during years with
65 good yields due to rising mean yields, years with adverse weather conditions do not experience benefit from additional
66 nutrient inputs. Studies with unequal effects and varying spatial scales show that there is potentially high subnational
67 heterogeneity in both yield variation as well as anthropogenic indicators. While the previous studies have been
68 conducted on diverse spatial scales (from villages to country and global level), only one global study (Simelton et al.,
69 2012) is linking multiple anthropogenic and production related indicators to crop yield variation, done using national
70 scale data.

71

72 In this study, we shed light on the abovementioned vulnerability issue and its implications for resilience by focusing
73 on crop yield variation and anthropogenic indicators on a subnational scale. More specifically, we examine 1) to what
74 level long-term averages of selected anthropogenic indicators (see Data and methods) can explain negative crop yield
75 variation, and 2) how well the anthropogenic indicators explain geographical differences in crop yield anomalies in
76 responses to heat and drought shocks. We utilized XGBoost algorithm to create regression models where the response
77 variable was observed crop yield data disaggregated to grid-level, and the explanatory variables were mostly
78 subnational or higher resolution anthropogenic indicators; a considerable enhancement from using national scale data
79 as done in existing studies. We used these global gridded datasets to study the relationship between anthropogenic
80 indicators and the yield variation of four key crops: wheat, maize, soybeans and rice. The wheat, maize, soybean and
81 rice are globally major staple crops covering 65% of global calorie intake (Tilman et al., 2011), with soybeans used
82 also extensively as feed for livestock (Hartman et al., 2011). In addition, these crops cover slightly more than 25% of
83 global food trade in terms of monetary values (MacDonald et al., 2015), thus having impact also on food security
84 through global trade networks and for providing income for farmers.

85

86 **2 Data and methods**

87 In this study, we focus on six key societal and crop production related indicators: i) Human Development Index, ii)
88 governance effectiveness, iii) fertilizer use (nitrogen, phosphorous and potassium), iv) water stress, v) irrigation and
89 vi) agricultural suitability for growing crops (see Table 1). Here we refer to these socio-economic and food production
90 indicators as “anthropogenic indicators” as they represent the human dimension controlling crop production. Unlike
91 e.g. climatic factors, these can potentially be influenced and controlled by human actions and policies.

92

93 To study the differences among distinct climatic systems, we split the data into six geographical areas using Holdridge
94 Life Zones that are based on three key climatological factors controlling crop production (precipitation,
95 biotemperature, and aridity) (Holdridge, 1947; Holdridge, 1967; Kummu et al., 2021). We combined the original 38
96 Holdridge Life Zones into six zones with similar climatic characteristics: “Cool”, “Temperate”, “Steppe”, “Arid”,
97 “Sub tropical”, and “Humid tropical” (see Fig. S1). We then analysed the association between crop yield anomalies
98 and the six indicators on 0.5 degree (~60 km at the equator) grid cell resolution with a gradient boosting regression
99 algorithm XGBoost (T. Chen & Guestrin, 2016). This was used for three cases: *yield loss risk* for years 1981-2009
100 and *shock factor*-cases for “hot” and “dry” years. Data and methods are described in more detail below.

101

102 2.1 Data

103 2.1.1 Crop yield data

104 For the crop yield and harvested area data, we used rasterised (0.5 degree resolution) maize, rice, soybean and wheat
105 annual yield and harvested area data (Ray et al., 2019) for years 1981-2009. The crop data from Ray *et al* (2019) is
106 procured from census observations from around 20'000 political units and gaps within reported data is filled with 5-
107 year averages. The crop yield dataset has been widely used in crop yield variation studies (e.g., Ray *et al* 2012, 2015,
108 2019, Vogel *et al* 2019).

109

110

111 *Table 1 Description of the data used in the study and their sources.*

Data name	Abbreviation	Description	Source
Holdridge Life Zones	HLZ	Produced by monthly climate data averaged over 1970-2000 (WorldClim v.2.1)	Kummu <i>et al</i> (2021)
Crop yield data			
Crop-specific annual yield and harvested area		Gridded data at 0.5 degree resolution. Data for years 1981-2009	Ray <i>et al</i> (2019)
Anthropogenic indicators			
Human Development Index	HDI	Subnational level HDI. 5 arc-minute raster; years 1995-2005	Smits and Permanyer (2019), data gaps filled using method from Kummu, Taka and Guillaume, (2018)
Governance effectiveness	GOV	5 arc-minute raster, national scale; years 1995-2005	WGI (2018)
Water stress	WS	Baseline water stress index 0-1; vector data with HydroBASINS6 resolution (Lehner & Grill, 2013)	Hofste <i>et al</i> (2019)
Irrigation infrastructure	WINF	Historical Irrigation Dataset of area equipped for irrigation: 5 arc-min raster, 1995-2005 in 5-year timesteps.	Siebert <i>et al</i> (2015)
Fertilizer use	FER	Crop-specific application rates of nitrogen, phosphorus, potassium; 5 arcmin raster, around year 2000	Mueller <i>et al</i> (2012), West <i>et al</i> (2014)
Suitability index	SI	Crop specific agro-climatic potential yields combined with soil/terrain data (GAEZ v3); 30 arc-min raster	Fischer <i>et al</i> (2012)
Temperature and soil moisture data			
Air temperature (°C)		Daily minimum and maximum temperature for years 1981-2009; re-gridded from 0.25 to 0.5 degree	AgMERRA reanalysis dataset by Ruane <i>et al</i> (2015)
Daily soil moisture (m ³ /m ³)		Soil moisture attained at 12:00 as the daily estimate for soil moisture for years 1981-2009; re-gridded from 0.28 to 0.5 degree	ERA5 re-analysis dataset by Hersbach <i>et al</i> (2020)

112

113

114 2.1.2 Anthropogenic indicators

115 For the socio-economic data we used two indicators: Human Development Index (HDI) at subnational level (Smits &

116 Permanyer, 2019) and national-level governance effectiveness (GOV; WGI 2018, Varis *et al* 2019). The gaps in HDI

117 data were filled by using a method from (Kummu et al., 2018). Both indicators were rasterised to 5 arc-minute
118 resolution spanning over 1990-2015.

119

120 To assess the use of water resources we used baseline water stress (WS; Hofste *et al.*, 2019) and area equipped for
121 irrigation (WINF; Siebert *et al.* 2015). Baseline water stress, i.e., average water withdrawals per available renewable
122 surface and ground water supplies for the time period 1960-2014, was used as the indicator for local pressure on water
123 use on hydrological subbasin level (HydroBASINS6). For fertilizer use (FER) we included a linear combination of
124 crop-specific gridded application rates for three main fertilizer components: nitrogen, phosphorous and potassium
125 (Mueller et al., 2012; West et al., 2014). These fertilizer fractions were combined using principal component analysis
126 (PCA) with rasterPCA-function from RStoolbox – package (Leutner et al., 2019) in RStudio (RStudio Team, 2019),
127 and the first component (highest variance explained) was used as an explanatory variable in the model. The reference
128 year is mostly year 2000 whereas some data are collected between 1994-2001. Although the dataset provides only a
129 snapshot for fertilizer application rates, to our knowledge there are no globally comprehensive timeseries on gridded
130 fertilizer application rates. Furthermore, while changes in fertilizer application rates for some countries have changed
131 substantially (especially in Southern Asia), the overall trend seems to be less drastic (Lu & Tian, 2017).

132

133 Suitability Index (SI) was extracted from FAO Global Agro-Ecological Zones (GAEZ) (Fischer et al., 2012). It aims
134 to capture how suitable areas are to crop-specific cultivation based on different management practices and a set of
135 environmental indicators, such as soil and terrain-slope conditions. Here, we utilized the crop specific global SI-raster
136 with intermediate-level of inputs.

137

138 All the indicator datasets were rasterised and aggregated to 0.5 degree resolution (Fig. 1). Due to the lack of
139 comprehensive timeseries data for several of the indicators, we used a raster cell specific average between 1995-2005
140 (where applicable, see Table 1) as a representative value for the whole time period. This may skew our results as some
141 countries have experienced major economic growth and societal changes within our study period. However, globally
142 the change for several indicators have been relatively modest (see e.g., Fig. S2 for subnational HDI). The selected
143 time period of 1995-2005 represents roughly the middle point of crop yield data (1981-2009). To diminish the impact
144 of outliers, all data were normalized between 2.5 and 97.5% of the respective ranges. The distributions and variable
145 correlations are presented in Fig. S3.

146

147 2.1.3 Temperature and soil moisture data

148 Abiotic stresses caused by extreme climatic events such as prolonged periods of high temperatures (here used as “hot”
149 shocks) or low soil moisture (“dry” shocks) can cause worsening conditions for crop growth through interference of
150 multiple factors such as nutrient and water balance, photosynthesis or assimilate partitioning (Fahad et al., 2017).
151 Here, we utilize air temperature (Ruane et al., 2015) and soil moisture (Hersbach et al., 2020) anomalies to study the
152 links between crop yields and anthropogenic indicators during so called “shock years”, as defined below.

153

154 To account for the intraday variation in temperature data, the daily temperatures were assumed to follow sine-function
155 so that daily minimum and maximum temperature was the lowest and highest daily value, respectively. The amplitude
156 of the variation was half of the difference between the daily low and high temperatures. For the daily soil moisture,
157 the hourly soil moisture attained at 12:00 in the ERA5 data set was used as the daily estimate for soil moisture. To
158 account for the different soil conditions globally, we standardized and transformed the data to relative soil moisture
159 deficit. This transformation was done for each raster cell by subtracting daily values from the cell specific maximum
160 reported daily soil moisture value for the whole time period and then dividing by the difference between minimum
161 and maximum reported daily soil moistures.

162

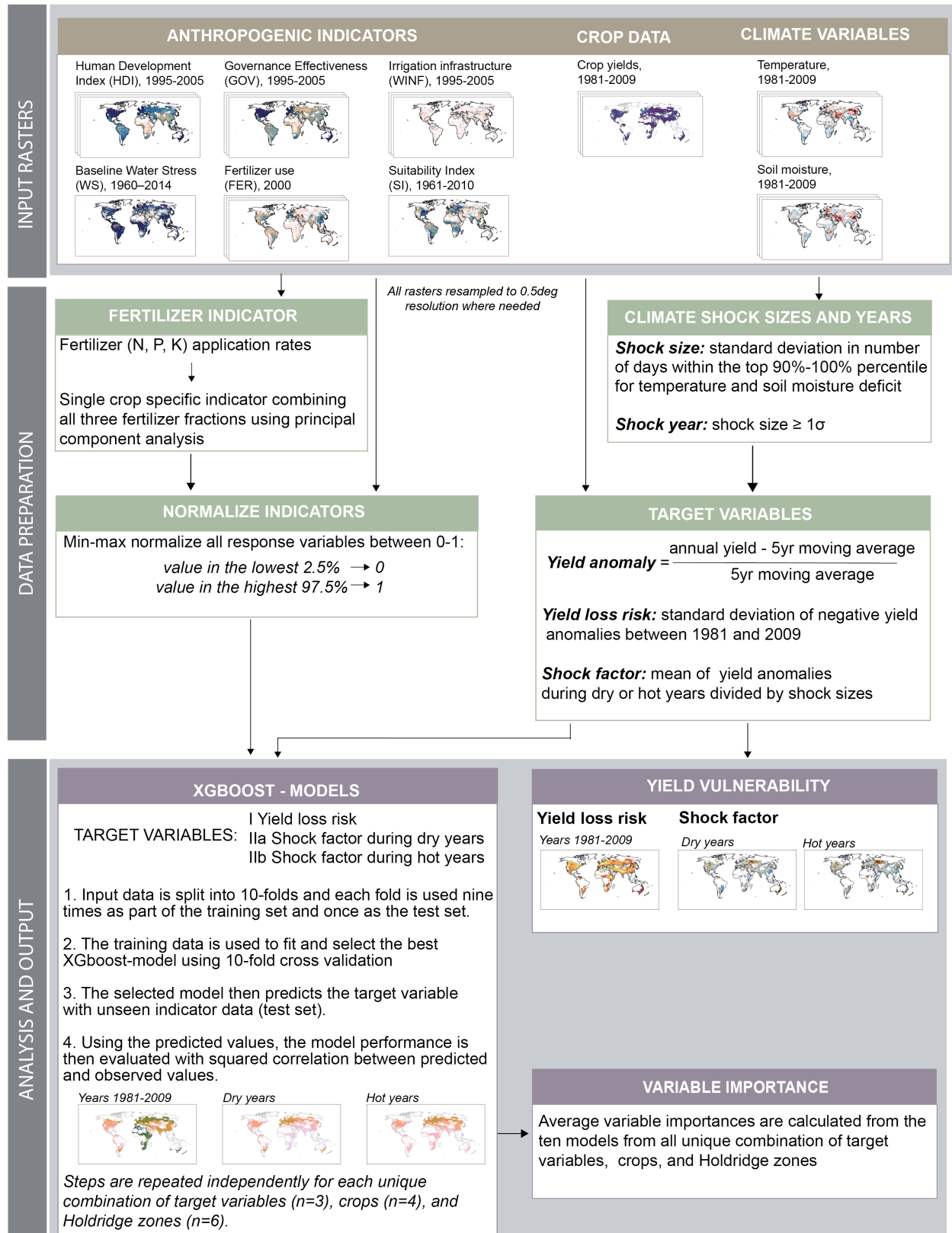
163 Both temperature (0.25 degrees) and soil moisture (0.28) datasets were re-gridded to 0.5 degree resolution:
164 temperature data were resampled using bilinear interpolation and the soil moisture data with piecewise linear
165 interpolation. We used data from years 1981-2009 for both datasets. More detailed description of the method for
166 temperature and soil moisture data manipulation is shown in Heino *et al.* (2021).

167

168

169 2.2 Methods

170 The general methodological framework is presented in Fig. 1, while more detailed description of the methods is
171 given below.



172

173

174

Figure 1 Conceptual methodological framework. More detailed descriptions of the data sources and methods can be found in Sections 2.1 Data and 2.2 Methods.

175

176 2.2.1 Yield loss risk

177 For studying the interannual variation in the yield anomalies, the annual absolute yields for each grid cell were first
178 detrended by subtracting the running 5-year mean from the annual yields. Then these detrended yields were divided
179 by the running 5-year mean of the annual yields to obtain comparable yield anomalies for each grid cell. The
180 prevalence of the yield data is relatively stationary across the whole time-period as most of the grid cells have yield
181 data for almost the whole study period.

182

183 The yield loss risk portrays the variation in loss events and is defined here as the standard deviation of negative yield
184 anomalies within each grid cell across years 1981-2009. Higher yield loss risk in a given grid cell depicts larger extent
185 of negative yield anomalies, i.e., higher losses in terms of annual yield. To obtain more representative yield loss risk,
186 we removed all grid cells with less than 15 crop specific observations to limit the potential outliers in areas where
187 extent of crop cultivation varies substantially from year to year. The sample sizes used for each Holdridge zone and
188 crop combination as well as the distribution of the yield loss risk values are shown in Fig. S4.

189

190 2.2.2 Shock factor

191 To study the effect of extreme temperature and soil moisture anomalies on yields, we used two distinct cases: “hot
192 years” denotes years with high temperatures and “dry years” those with very low soil moisture (Fig. 1). The extent of
193 the anomalies was measured within each grid cell that fall above 90th percentile threshold for temperature and soil
194 moisture deficit. Only years when the number of days was over one standard deviation higher compared to the cell
195 specific mean (“hot” or “dry” years) were included in the shock models. Both cases were considered separately, thus
196 a single year can belong into “hot”, “dry” or both categories. For more detailed description of calculating the “hot” or
197 “dry” conditions, see Heino *et al* (2021).

198

199 Both the temperature and soil moisture conditions have substantial interannual variation. To make the yield effects of
200 the anomalies comparable for each grid cell-year pair, the absolute crop yield anomalies were scaled using the shock
201 size, i.e., standard deviation in the number dry or hot days for a given year. Thus, a grid cell (0.5 degree) with similar
202 crop yield anomalies, a year with higher *temperature or soil moisture* anomaly would receive a lower (closer to zero)
203 value compared to year with lower anomaly. The sample sizes used for each Holdridge zone and crop combination as
204 well as the distribution of the outcome values for “hot” and “dry” cases are shown in Fig. S5 and the unadjusted mean
205 yield anomalies during shock years are presented in Fig. S6.

206

207 2.2.3 Modelling setup

208 We used predictive regression models to study the explanatory power of the anthropogenic indicators on crop yield
209 anomalies. The models were built using gradient boosting algorithm XGBoost (T. Chen & Guestrin, 2016) which
210 implements a non-parametric ensemble machine learning method utilizing weak learners, e.g., decision trees for

211 various regression and classification tasks (Friedman, 2001). Decision tree models are generally well suited to detect
212 non-linear relationships such as crop yields (Leng & Hall, 2020), as well as handle multicollinear variables, and they
213 do not require assumptions on the distributions (e.g., assumption of normality) of the input data. This enables us to
214 use data with non-normally distributed data (see Figs. S3-S5). In this study, the model implementation including model
215 tuning and predictions was done using *xgboost*- and *caret*-packages (T. Chen et al., 2021; Kuhn, 2020) in R software
216 (R Core Team, 2020).

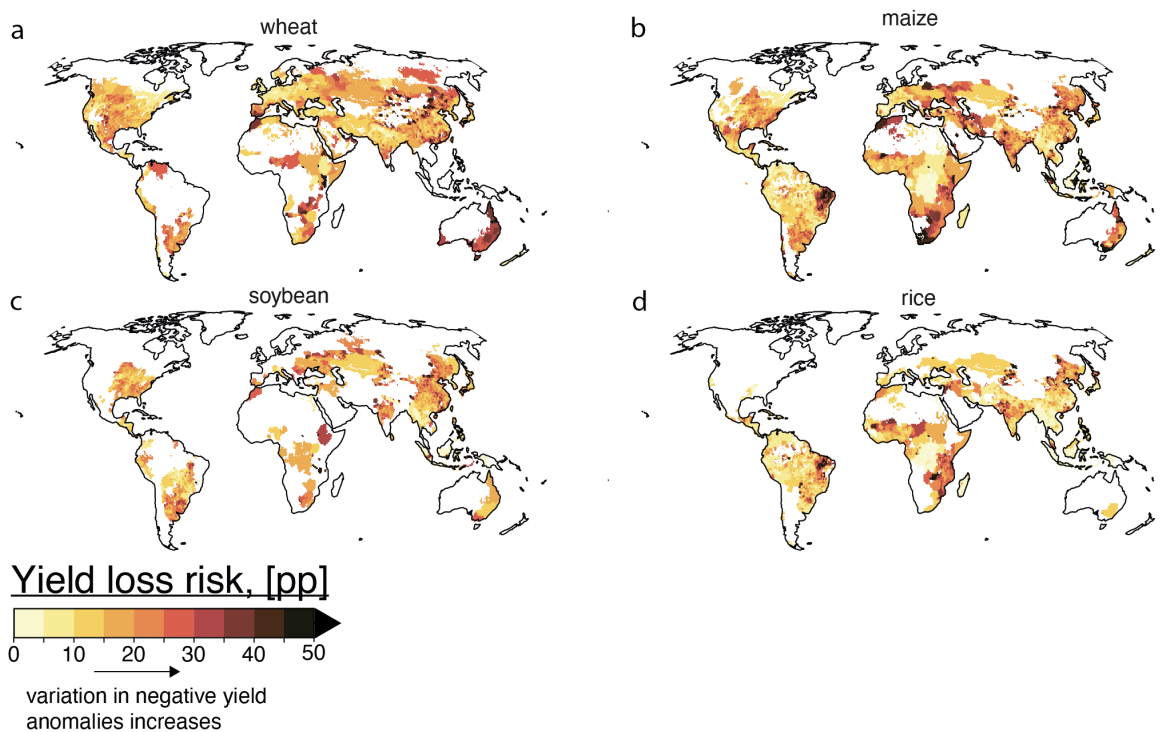
217
218 We did three separate analyses looking at the association between crop yield variability and anthropogenic indicators
219 with different outcome variables: yield loss risk and shock factors for “hot” and “dry” years (see Sections 2.2.1 and
220 2.2.2). For all outcome variables, the regressions were run separately for each Holdridge zone and crops to estimate
221 the importance of the different variables in areas with similar climatic conditions. Holdridge zones with less than 250
222 observations (i.e., grid cells with data for all indicators) were excluded from the analysis. The performance of the
223 models was assessed using the squared Pearson correlation coefficient (sign preserved) between the observed and
224 predicted outcomes.

225
226 Similarity in observation caused by spatial autocorrelation can cause training and test sets to become similar if assigned
227 randomly. This can lead to overly optimistic performance estimates, when in reality the good performance comes from
228 overfitting (Meyer et al., 2019). To combat this issue in the training and test sets, we first split the grid points into
229 small batches using global 100 x 100 hexagon grid with majority of hexagons covering 40-50 adjacent grid cells. All
230 the grid cells within a single hexagon are assigned to the same training or test sets. We then used a nested cross-
231 validation (CV) where first the outer CV splits the data into 10 folds with no overlapping grid points and uses each
232 fold once for evaluating the model chosen in the inner CV loop. The outer cross-validation loop feeds nine folds to
233 the inner CV that performs also 10-fold cross-validation to tune the hyperparameters using grid search with default
234 settings in *caret*-package. The hyperparameter combination with the lowest root mean squared error was chosen.
235 Accordingly, for each Holdridge zone, the outcome variable in a given grid cell was predicted using one of the 10
236 chosen models that did not use said grid point in the training phase.

237
238 To analyse the importance of the variables, we used *xgb.importance*-function from *xgboost*-package (T. Chen et al.,
239 2021). The importance was measured as Gain-values, which indicates how the inclusion of a variable within a certain
240 split of the boosted tree model improves the accuracy of the prediction. Higher Gain-value indicate that the variable
241 was more important for the prediction. Using the variable importance, however, comes with a few caveats. Firstly, the
242 importance does not reveal the actual direction of the relationship between a variable and the outcome variable.
243 Secondly, collinear variables might not have accurate Gain-values as the models can “prefer” one of the collinear
244 variables by putting more weight on the same variable at each split while disregarding the other collinear variables (T.
245 Chen et al., 2018). To supplement the variable importance and to measure the direction of the relationships, we utilize
246 accumulated local effects –visualization (ALE) that provides a method to assess the marginal effects different
247 indicators have on the outcome variables (Apley & Zhu, 2020).

248 **3 Results**249 **3.1 Yield loss risk**

250 We found substantial geographical distinctiveness when assessing the yield loss risk on each grid cell (Fig. 2). For
 251 wheat, the strongest negative anomalies occur in a major wheat producer country Australia, as well as North-eastern
 252 China and various parts of Africa (Fig. 2a). For maize and rice, the spatial pattern is somewhat similar, as largest risks
 253 occur in North-eastern Brazil, Southern Africa, Morocco, Middle East and parts of Central Asia (Fig. 2b, d). When
 254 comparing the values with the mean yield loss risks of respective Holdridge zones, especially Africa shows several
 255 hotspots for wheat, maize, and rice with over 20 percentage points higher risk for yield loss compared to the respective
 256 zone's mean value (Fig. S7). For soybean, while having lower yield loss risks, the most vulnerable areas were found
 257 in North-eastern China, eastern Europe and central Asia, Ethiopia as well as Uruguay and Northern Argentina (Fig.
 258 2c).



259

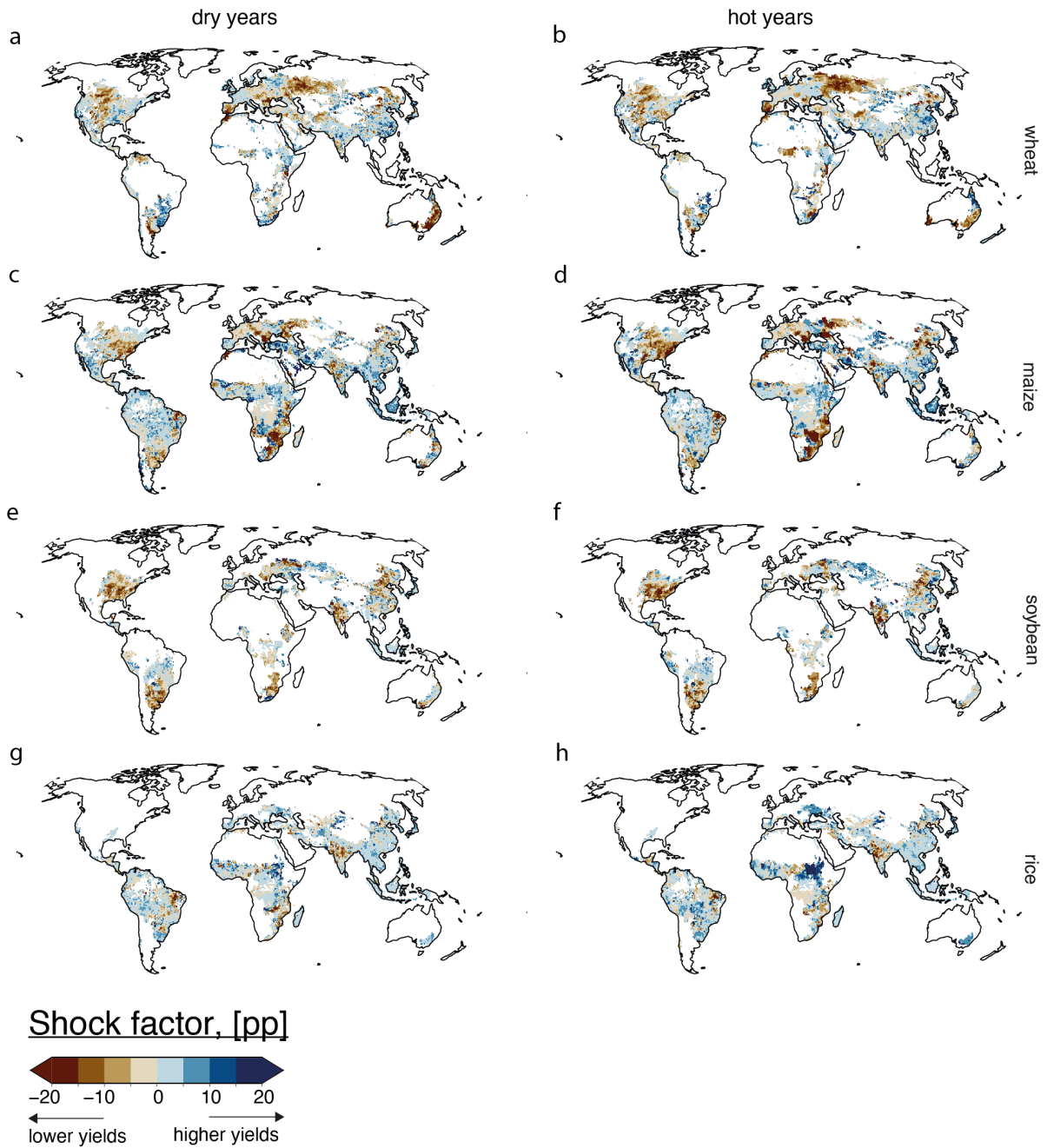
260 *Figure 2 Yield loss risk, i.e., standard deviation of negative yield anomalies measured for a. wheat, b. maize, c. soybean, and d.*
 261 *rice. Increasing yield loss risk indicates that a grid cell has larger negative yield anomalies (i.e., yields lower than 5-year*
 262 *average) during the study period. In other words, areas with higher yield loss risk experience worse negative yield anomalies*
 263 *than areas with lower yield loss risk. White areas indicate no production of the crop in question.*

264

265 **3.2 Shock factor**

266 When considering only the climatic shock, i.e. dry and hot years (see Methods), our findings highlight those areas
 267 with highest crop yield anomaly during shock years (Fig. 3; scaled so that comparable between grid cells; see Methods)

268 are mainly same as those where the yield loss risk is the highest (Fig. 2). For example, the strongest negative yield
269 anomaly for wheat during dry years (Fig. 3a) are found in Australia, similar to the yield loss risk (Fig. 3a). Also,
270 Eastern Europe and Central Asia as well as parts of Midwestern Northern America shows high negative shock factor
271 for wheat (Fig. 3a, b) and maize (Fig. 3c, d). Eastern United States and Southern parts of Latin America have the
272 highest negative impacts in soybean cultivation from both hot and dry shocks. For rice, (Fig. 3g, h) there seems to be
273 much less geographical variation and generally lower negative shock factors than the other crops, in line with previous
274 studies where climatic conditions have been found to have lower effects for rice compared to other crops (e.g., Ray *et*
275 *al* 2015). When comparing the shock factors to the mean of respective Holdridge zones (Fig. S8), all the studied crops
276 show similar geographical patterns as in absolute shock factor values (Fig. 3) indicating that the mean effect across
277 each of the climatic zones is rather minor (Fig. S9).



278

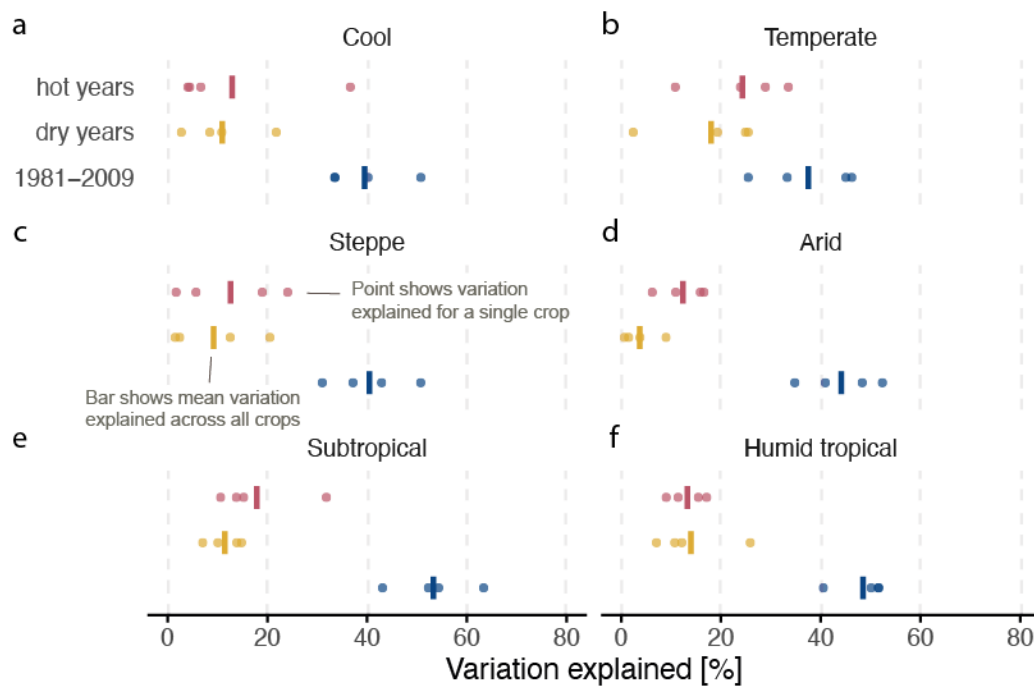
279 *Figure 3 Mean yield anomalies during shock years adjusted by shock size. The sign of the shock factor indicates whether the*
 280 *mean yields for shock years are higher (positive values; blue) or lower (negative values; brown) than the running 5-year mean*
 281 *yield. The size of the shock factor indicates how large the shock size adjusted yield anomaly is during shock years. Dry years are*
 282 *those when number of days with soil moisture deficit in the >90th percentile is more than 1 standard deviation from the long-term*
 283 *mean. Hot years indicate that the number of days when number of days with air temperature in the >90th percentile is more than*
 284 *1 standard deviation from the long-term mean.*

285

286 3.3 Explanatory power of anthropogenic indicators

287 Anthropogenic indicators had substantially higher explanatory power in *yield loss risk* -case compared to when only
 288 shock years, either “dry” or “hot”, were examined (Fig. 4). This applies to all the studied crops and Holdridge climate
 289 zones. For the yield loss risk -case, the explanatory power of the models across both the crops and Holdridge zones
 290 seem to be quite clustered, whereas for the shock cases, especially hot years have somewhat larger range of values
 291 with regards to the explanatory power of the models (e.g., Cool, Temperate, Steppe and Subtropical zones: Fig. 4a, b,
 292 c, e). The mean explanatory power for yield loss risk varied generally between 40-60%, depending on climate zone
 293 (Fig. 4) and crop (Fig. 5), whereas the mean explained variation in shock years was substantially lower, around 5 to
 294 20%.

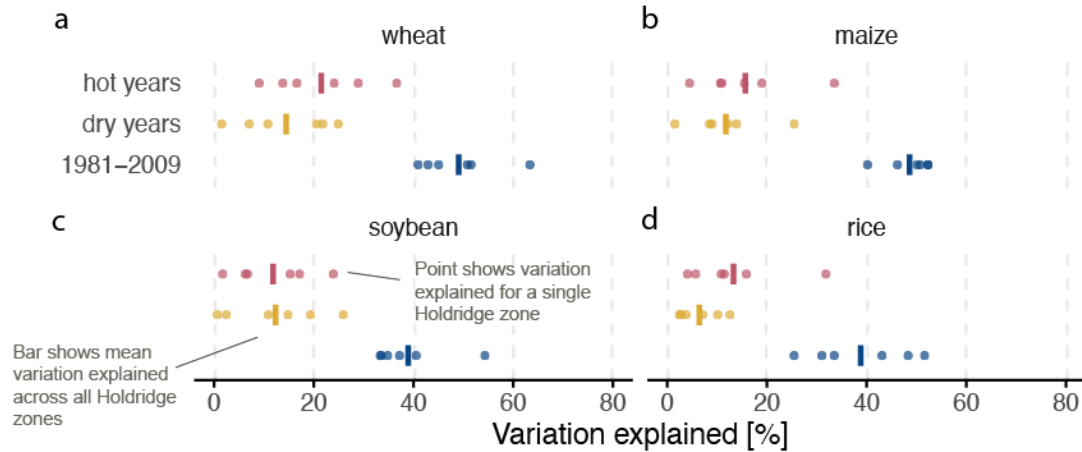
295



296

297 *Figure 4 Variation explained within different Holdridge zones. Blue colour represents yield loss risk -case for years 1981-2009,*
 298 *and yellow and red colours represent shock factor -cases for dry and hot years, respectively (see Methods). Each point represents*
 299 *variation explained by models for single crop and horizontal bars represent the mean explanatory power across all crops.*
 300 *Explained variation is measured as the squared Pearson's correlation coefficient between the observed and predicted outcome.*

301 The explanatory power for yield loss risk in years 1981-2009 was rather similar (in average around 40-50%) across
 302 all crops (Fig. 4). The best model performance in explaining the yield loss risk was observed in Subtropical and Humid
 303 tropical climate zones (ca 50-55% on average), and lowest in Cool and Temperate zones (around 40%) (Fig. 4). In
 304 terms of hot/dry shock years only, the mean shock factors were usually better explained in hot years, the difference to
 305 dry years being in average 5-10 percentage points. For the crops, wheat models (Fig. 5a) had the largest mean
 306 explanatory power for hot years (around 20%) while the mean value for dry years was around 10% for wheat, maize
 307 and soybean and lower for rice (Fig. 5).

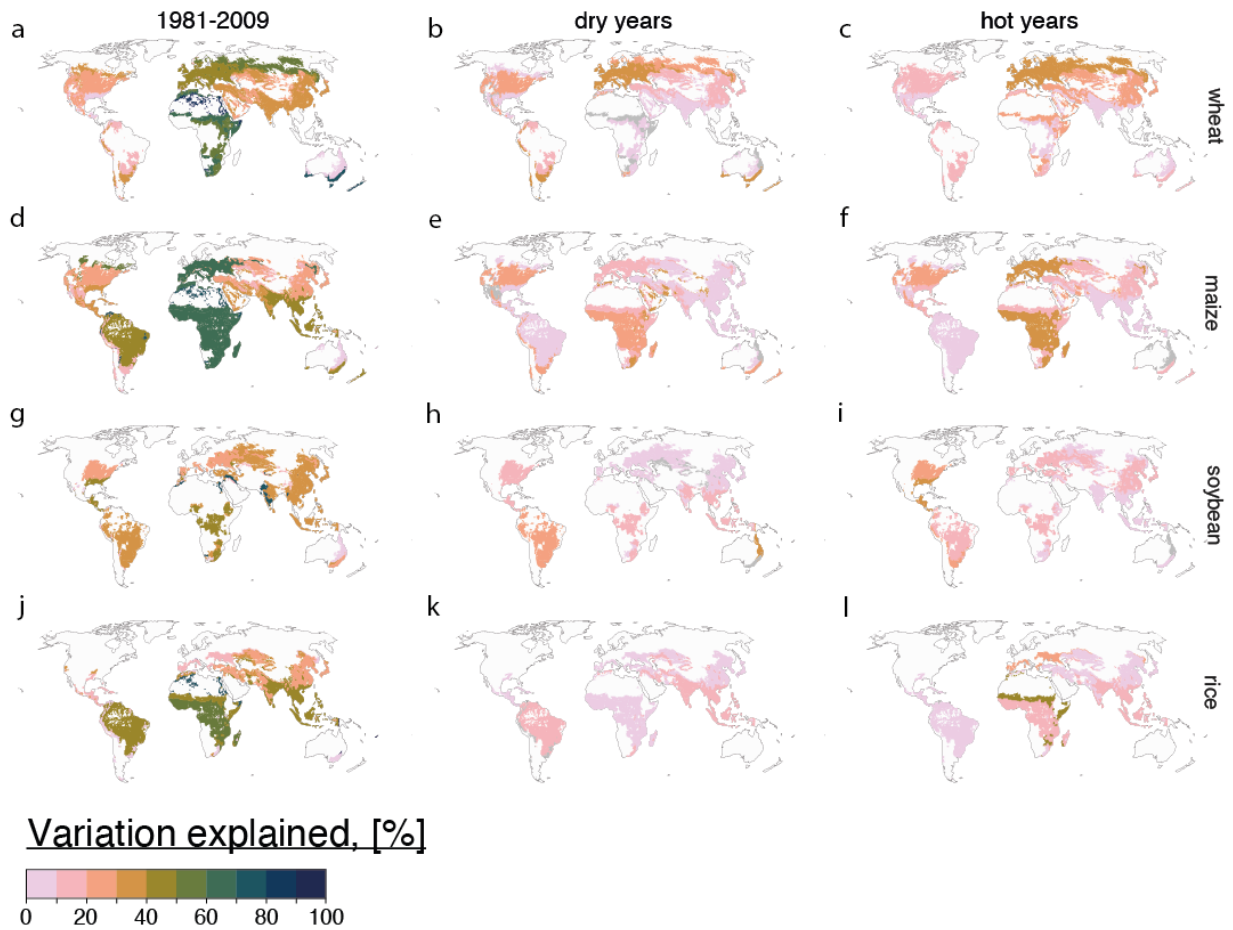


308

309 *Figure 5 Variation explained for different crops. Blue colour represents yield loss risk -case for years 1981-2009, and yellow and*
 310 *red colours represent shock factor -cases for dry and hot years, respectively (see Methods). Each point represents variation*
 311 *explained by models for single Holdridge zone and horizontal bars represent the mean explanatory power across all Holdridge*
 312 *zones. Explained variation is measured as the squared Pearson's correlation coefficient between the observed and predicted*
 313 *outcome.*

314 Measuring the explained variation for intersections of Holdridge zones and continents shows substantial geographical
 315 variation for all the crops in the *yield loss risk* -case (Fig. 6). In majority of Africa, for example, the explained variation
 316 was above 50% for all the crops. For the temperate regions in Europe and United States the fitted models explained
 317 over 40% of the variation for wheat (Fig. 6a) and maize (Fig. 6d). By contrast, for the majority of the areas, the models
 318 captured less than 30% of the variation in mean yield anomalies during shock years. Only wheat (Fig. 6c) and maize
 319 (Fig. 6f) models in the Temperate Holdridge zones during hot years performed better, having explanatory power over
 320 40%. The explanatory power was particularly low, for both dry and hot years, for areas in Latin America and East
 321 Asia.

322



323

324 *Figure 6 Explanatory power of the models within intersection of each Holdridge zone and continents for each crop (n = 37-42).*325 *Explained variation is measured as the squared Pearson's correlation coefficient between the observed and predicted outcome.*326

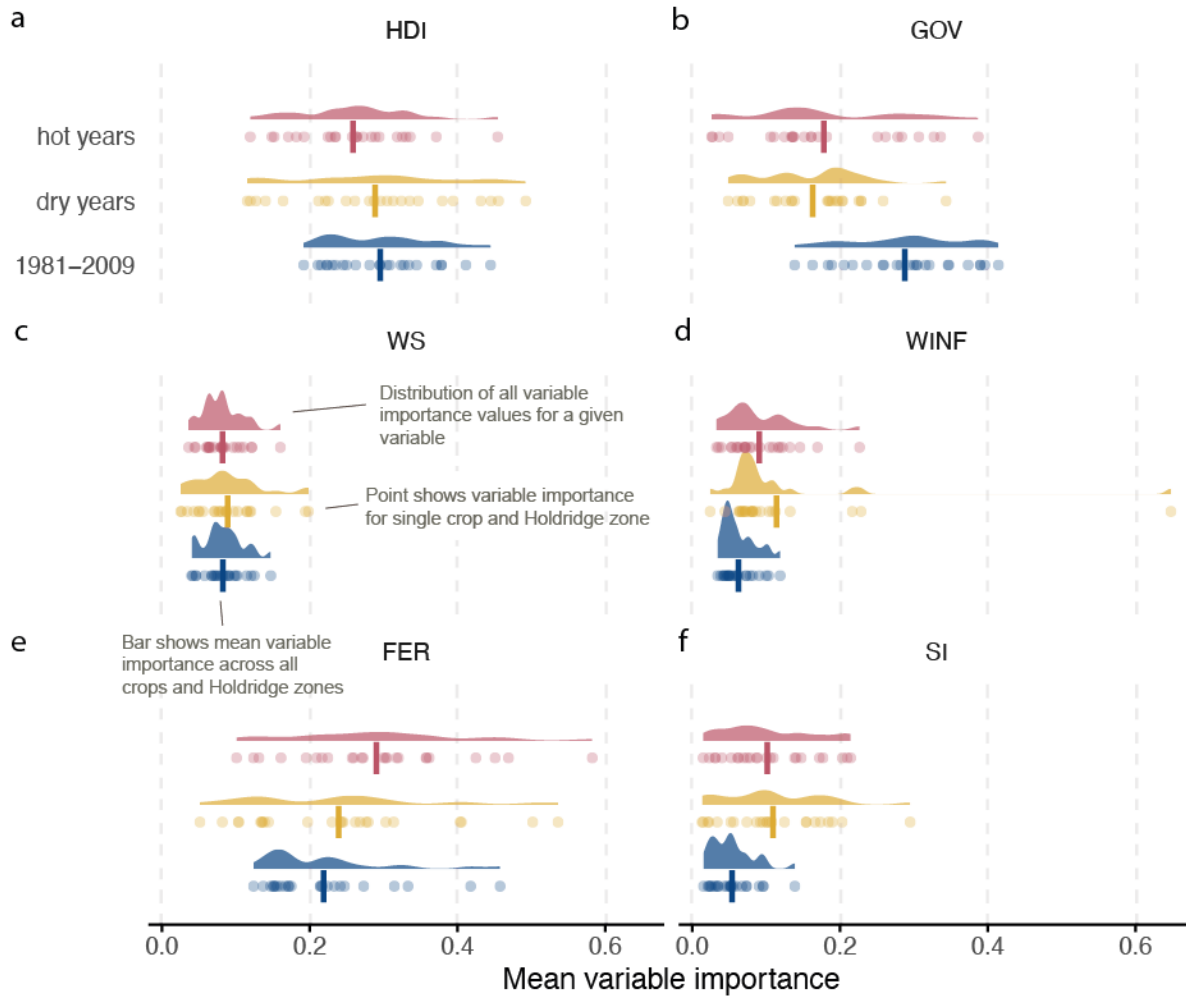
3.4 Importance of anthropogenic indicators

327 On global average, the most important predicting indicators were Human Development Index (HDI), governance
 328 (GOV) and fertilizer use (FER) (Fig. 7). However, these indicators, especially FER, also had the highest range in
 329 importance values across different crops and climate zones (Fig. 7e). When comparing the shock years to the general
 330 yield loss case, some interesting differences were observed: the socio-economic indicators (HDI, GOV) had higher
 331 importance in yield loss case than shock years, while for all other indicators, except for WS with no difference, the
 332 relationship is the opposite (Fig. 7). The difference is particularly strong in case of GOV, which is much more
 333 important in yield loss case than in shock case. This indicates that the importance of different anthropogenic indicators
 334 is different in 'normal' conditions than shock conditions.

335

336 When assessing the direction of the association between the indicators and the yield loss risk, indicators such as HDI
 337 or FER had quite varying impacts within different Holdridge zones (Fig. S10). Quite unsurprisingly, higher fertilizer

338 use seems to contribute to lower yield variability for all the Holdridge zones with the exception for a few areas such
 339 as steppe for maize and soybean and subtropical for wheat. For HDI, the relationships between the indicator value and
 340 modelled variation were often nonlinear. Increasing of HDI over the 0.5 normalized HDI (i.e., half of the maximum
 341 HDI value) seems to yield substantially less variation in yield loss risk (Fig. S10).
 342



343
 344 *Figure 7 Mean variable importance for each indicator. The indicators included are a. Human Development Index (HDI), b.*
 345 *Governance efficiency (GOV), c. water stress (WS), d. irrigation infrastructure (WINF), e. fertilizer use (FER) and f.*
 346 *Suitability index (SI). Variable importance is measured as mean Gain-values of models (n=10) for a given crop (n=4) and*
 347 *Holdridge zone combination (n=24). Higher Gain-value indicates that the variable is more important making the prediction.*
 348 *Blue colour represents yield loss risk -case for years 1981-2009, and yellow and red colours represent shock factor -cases for*
 349 *dry and hot years, respectively (see Methods). Each point represents variable importance for single model for a given crop and*
 350 *Holdridge zone, the distribution shows how tightly clustered the variable importance values are, and horizontal bars represent*
 351 *the mean explanatory power across all crops and Holdridge zones.*

352

353 4 Discussion and conclusions

354 4.1 Key findings

355 We studied crop yield vulnerabilities and their relationship to global socioeconomic indicators with three specific
356 cases. First, we focused on yield variation measured as standard deviation of the negative yield anomalies (*yield loss*
357 *risk -case*). In the other cases, we considered mean yield anomalies during shock years only (hot years for high
358 temperature and dry years for high soil moisture deficit). Our results suggest that the long-term mean of the selected
359 anthropogenic indicators has substantial explanatory power over the variation of negative yield anomalies within
360 different climatological contexts (Fig 4. and Fig. 6). While the indicators used here are not necessarily directly linked
361 to different adaptation capabilities, they seem to have clear association with the yield variation for most of the studied
362 crops and Holdridge climatic zones.

363
364 When using mean yield anomalies during shock years as the target variable, the explanatory power is noticeably lower
365 than in yield loss risk -case (Fig. 3 and Fig. 4). One potential reason for the difference is that the indicators with only
366 a single long-term average for a given indicator cannot capture the potential for adaption measures that are employed
367 on farm level during the shock years. The farm-level management decisions together with sufficient regional diversity
368 in farm characteristics can reduce the regional impacts of climate related shocks (Reidsma et al., 2010). In addition,
369 decision to employ adaptation measures can depend on many factors, such as cultivated crop type (grain or cash crop),
370 education level, access to electricity for irrigation, or access to credit (Alauddin & Sarker, 2014; Bryan et al., 2009;
371 H. Chen et al., 2014). With generic indicators such as HDI we cannot differentiate the actual locations where
372 adaptation methods are utilized.

373
374 The most important indicators support the fact that areas with increasing HDI and fertilizer use values have lower
375 negative yield variation which supports also findings of existing studies (Antwi-Agyei et al., 2012; Kamali et al.,
376 2019; Simelton et al., 2012). However, the relationship between different indicators and yield variability is not
377 straightforward in many areas. For example, HDI and yield variation had a convex relationship as areas with low and
378 high HDI have considerably lower yield loss risk compared the “middle-ground” areas (Fig. S10). Studies such as
379 Reidsma *et al.* (2010) and Bharwani *et al.* (2005) suggest that poorer farmers might be better at adapting to climate
380 variability compared to richer farmers who respond more actively to market signals rather than climate signals.
381 Simelton *et al.* (2012), who also observed similar results, hypothesized that farmers in poorer countries relied on more
382 traditional farming and adaptation methods which are no longer utilized when country moves from poor to middle-
383 incoming country, thus increasing drought vulnerability.

384
385 Surprisingly, irrigation infrastructure (WINF) was relatively unimportant indicator for the predictions (Fig. 7) even
386 though it has been previously identified as major factor reducing crop yield variation as well as buffer against extreme
387 warm days (Butler & Huybers, 2013; Troy et al., 2015; Vogel et al., 2019). The dataset used here (Siebert et al., 2015)
388 is not crop specific, thus detecting effects of irrigation for a certain crop may be challenging. While we used same

389 irrigation infrastructure extent for all the crops, there are major differences where irrigation is used with a given crop
390 (Portmann et al., 2010), creating noise in the model.

391

392 4.2 Limitations and way forward

393 Assessing the relationship of crop yield anomalies and anthropogenic indicators on a global scale has several
394 challenges. Firstly, comprehensive global timeseries on farm-management practices that span sufficient long time
395 period are non-existent. Using long term mean values for indicators might not be representative for countries that have
396 experienced drastic changes during the study time period. Secondly, we employ a set of rather generic indicators which
397 might not correlate directly with the management practices and decision done in the farms. While generic indicators
398 such as gross domestic product or human development index are generally used as proxies for location specific
399 adaptive capacity, more specific political and socio-economic contexts are needed to measure the impacts of specific
400 interventions (Challinor et al., 2010). However, to our knowledge, comparable data on a global scale at subnational
401 or higher resolution does not exist. Further, crop responses may be highly non-linear compared to each other, (Jackson
402 et al., 2021), thus selecting an arbitrary shock threshold may have very different adaptation implications depending
403 on the crop in question. Also, additional environmental factors such as soil type may have substantial impacts on the
404 results (Folberth et al., 2016) further complicating the relationships.

405

406 4.3 Concluding remarks

407 The global food systems are facing increasing risks as the hot and dry conditions are getting more common (Sarhadi
408 et al., 2018). Further, the increasing shocks can affect multiple crops or crops within different “breadbaskets”
409 simultaneously (Gaupp et al., 2020; Tigchelaar et al., 2018) causing major challenges especially from food security
410 perspective if the lack of production cannot be compensated by trade. From a longer time perspective, climate change
411 is also pushing substantial size of the food production outside of the current. climatic conditions (Kummu et al., 2021).
412 These changes amplify the need for understanding local vulnerabilities across the globe. The results from our high-
413 resolution study indicate the most vulnerable crop production areas to negative crop yield variability, where
414 prioritizing the mitigation efforts could increase the local food security. While the variation in yields cannot be entirely
415 prevented, agricultural policies which support increasing local nutrient availability through nutrient recycling and
416 effective fertilizer use promote resilience towards shocks. In addition, proper social and institutional support as well
417 as understanding local contexts when developing the areas suffering from low education and poverty have important
418 contribution for supporting local food security.

419

420

421 **Acknowledgments, Samples, and Data**

422 The authors declare no conflicts of interest relevant to this study.

423 The study was funded by Maa- ja vesiteknikan tuki ry, Academy of Finland funded project WATVUL (grant no.
424 317320), Academy of Finland funded project TREFORM (grant no. 339834), and European Research Council (ERC)
425 under the European Union's Horizon 2020 research and innovation programme (grant agreement No. 819202). We
426 also thank Ilkka Mellin for his valuable comments on the methodology. DKR was supported by the Institute on the
427 Environment, University of Minnesota.

428

429 **Author contributions**

430 PK, MT, MK created initial study design. PK and MH were responsible for the analyses. DKR supplied crop yield
431 data. PK wrote the manuscript with contributions from, MH, MT, VS and MK.

432

433 **Code availability**

434 All the codes for creating the results in this paper are available at https://github.com/pskinnun/shock_vulnerability

435

436 **Data availability**

437 All raw data sources are open sourced and available online.

438

439 **References**

440 Alauddin, M., & Sarker, M. A. R. (2014). Climate change and farm-level adaptation decisions and strategies in
441 drought-prone and groundwater-depleted areas of Bangladesh: an empirical investigation. *Ecological Economics*,
442 *106*, 204–213. <https://doi.org/10.1016/j.ecolecon.2014.07.025>

443

444 Antwi-Agyei, P., Fraser, E. D. G., Dougill, A. J., Stringer, L. C., & Simelton, E. (2012). Mapping the vulnerability
445 of crop production to drought in Ghana using rainfall, yield and socioeconomic data. *Applied Geography*, *32*(2),
446 324–334. <https://doi.org/10.1016/j.apgeog.2011.06.010>

447

448 Apley, D. W., & Zhu, J. (2020). Visualizing the effects of predictor variables in black box supervised learning
449 models. *Journal of the Royal Statistical Society: Series B (Statistical Methodology)*, *82*(4), 1059–1086.

450 <https://doi.org/10.1111/rssb.12377>

451

452 Bharwani, S., Bithell, M., Downing, T. E., New, M., Washington, R., & Ziervogel, G. (2005). Multi-agent
453 modelling of climate outlooks and food security on a community garden scheme in Limpopo, South Africa.

454 *Philosophical Transactions of the Royal Society B: Biological Sciences*, *360*(1463), 2183–2194.

455 <https://doi.org/10.1098/rstb.2005.1742>

- 456
457 Bryan, E., Deressa, T. T., Gbetibouo, G. A., & Ringler, C. (2009). Adaptation to climate change in Ethiopia and
458 South Africa: options and constraints. *Environmental Science & Policy*, 12(4), 413–426.
459 <https://doi.org/10.1016/j.envsci.2008.11.002>
460
- 461 Butler, E. E., & Huybers, P. (2013). Adaptation of US maize to temperature variations. *Nature Climate Change*,
462 3(1), 68–72. <https://doi.org/10.1038/nclimate1585>
463
- 464 Challinor, A. J., Simelton, E. S., Fraser, E. D. G., Hemming, D., & Collins, M. (2010). Increased crop failure due to
465 climate change: assessing adaptation options using models and socio-economic data for wheat in China.
466 *Environmental Research Letters*, 5(3), 034012. <https://doi.org/10.1088/1748-9326/5/3/034012>
467
- 468 Chatzopoulos, T., Pérez Domínguez, I., Zampieri, M., & Toreti, A. (2020). Climate extremes and agricultural
469 commodity markets: A global economic analysis of regionally simulated events. *Weather and Climate Extremes*, 27,
470 100193. <https://doi.org/10.1016/j.wace.2019.100193>
471
- 472 Chen, H., Wang, J., & Huang, J. (2014). Policy support, social capital, and farmers' adaptation to drought in China.
473 *Global Environmental Change*, 24, 193–202. <https://doi.org/10.1016/j.gloenvcha.2013.11.010>
474
- 475 Chen, T., & Guestrin, C. (2016). XGBoost: A Scalable Tree Boosting System. In *Proceedings of the 22nd ACM*
476 *SIGKDD International Conference on Knowledge Discovery and Data Mining* (pp. 785–794). New York, NY,
477 USA: ACM. <https://doi.org/10.1145/2939672.2939785>
478
- 479 Chen, T., Benesty, M., & He, T. (2018). Understand Your Dataset with Xgboost. Retrieved July 6, 2021, from
480 [https://cran.r-project.org/web/packages/xgboost/vignettes/discoverYourData.html#numeric-v.s.-categorical-](https://cran.r-project.org/web/packages/xgboost/vignettes/discoverYourData.html#numeric-v.s.-categorical-variables)
481 [variables](https://cran.r-project.org/web/packages/xgboost/vignettes/discoverYourData.html#numeric-v.s.-categorical-variables)
482
- 483 Chen, T., He, T., Benesty, M., Khotilovich, V., Tang, Y., Cho, H., et al. (2021). *xgboost: Extreme Gradient*
484 *Boosting*. Retrieved from <https://CRAN.R-project.org/package=xgboost>
485
- 486 Cohn, A. S., Newton, P., Gil, J. D. B., Kuhl, L., Samberg, L., Ricciardi, V., et al. (2017). Smallholder Agriculture
487 and Climate Change. *Annual Review of Environment and Resources*, 42(1), 347–375.
488 <https://doi.org/10.1146/annurev-environ-102016-060946>
489
- 490 Cottrell, R. S., Nash, K. L., Halpern, B. S., Remenyi, T. A., Corney, S. P., Fleming, A., et al. (2019). Food
491 production shocks across land and sea. *Nature Sustainability*, 2(2), 130–137. [https://doi.org/10.1038/s41893-018-](https://doi.org/10.1038/s41893-018-0210-1)
492 [0210-1](https://doi.org/10.1038/s41893-018-0210-1)

493
494 Distefano, T., Laio, F., Ridolfi, L., & Schiavo, S. (2018). Shock transmission in the International Food Trade
495 Network. *PLOS ONE*, 13(8), e0200639. <https://doi.org/10.1371/journal.pone.0200639>
496
497 Fahad, S., Bajwa, A. A., Nazir, U., Anjum, S. A., Farooq, A., Zohaib, A., et al. (2017). Crop Production under
498 Drought and Heat Stress: Plant Responses and Management Options. *Frontiers in Plant Science*, 8, 1147.
499 <https://doi.org/10.3389/fpls.2017.01147>
500
501 FAO (Ed.). (2019). *Safeguarding against economic slowdowns and downturns*. Rome: FAO.
502
503 Fischer, G., Nachtergaele, F. O., Prieler, S., Teixeira, E., Toth, G., Velthuisen, H. van, et al. (2012). Global Agro-
504 ecological Zones (GAEZ v3.0)- Model Documentation. Laxenburg, Austria; Rome, Italy: IIASA, Laxenburg,
505 Austria and FAO, Rome, Italy. Retrieved from <http://pure.iiasa.ac.at/id/eprint/13290/>
506
507 Folberth, C., Skalský, R., Moltchanova, E., Balkovič, J., Azevedo, L. B., Obersteiner, M., & van der Velde, M.
508 (2016). Uncertainty in soil data can outweigh climate impact signals in global crop yield simulations. *Nature*
509 *Communications*, 7(1), 11872. <https://doi.org/10.1038/ncomms11872>
510
511 Friedman, J. H. (2001). Greedy function approximation: a gradient boosting machine. *Annals of Statistics*, 1189–
512 1232. <https://doi.org/10.1214/aos/1013203451>
513
514 Fuss, S., Havlík, P., Szolgayová, J., Schmid, E., Reuter, W. H., Khabarov, N., et al. (2015). Global food security &
515 adaptation under crop yield volatility. *Technological Forecasting and Social Change*, 98, 223–233.
516 <https://doi.org/10.1016/j.techfore.2015.03.019>
517
518 Gaupp, F., Hall, J., Hochrainer-Stigler, S., & Dadson, S. (2020). Changing risks of simultaneous global breadbasket
519 failure. *Nature Climate Change*, 10(1), 54–57. <https://doi.org/10.1038/s41558-019-0600-z>
520
521 Gbetibouo, G. A., Ringler, C., & Hassan, R. (2010). Vulnerability of the South African farming sector to climate
522 change and variability: An indicator approach. *Natural Resources Forum*, 34(3), 175–187.
523 <https://doi.org/10.1111/j.1477-8947.2010.01302.x>
524
525 Hartman, G. L., West, E. D., & Herman, T. K. (2011). Crops that feed the World 2. Soybean—worldwide
526 production, use, and constraints caused by pathogens and pests. *Food Security*, 3(1), 5–17.
527 <https://doi.org/10.1007/s12571-010-0108-x>
528

- 529 Heino, M., Kinnunen, P., Anderson, W., Ray, D., Puma, M. J., Varis, O., & Kummu, M. (2021). *Increased*
530 *probability of crop yield reducing hot and dry weather extremes*. Manuscript under preparation.
531
- 532 Hersbach, H., Bell, B., Berrisford, P., Hirahara, S., Horányi, A., Muñoz-Sabater, J., et al. (2020). The ERA5 global
533 reanalysis. *Quarterly Journal of the Royal Meteorological Society*, 146(730), g. <https://doi.org/10.1002/qj.3803>
534
- 535 Hofste, R. W., Kuzma, S., Walker, S., Sutanudjaja, E. H., Bierkens, M. F., Kuijper, M., et al. (2019). Aqueduct 3.0:
536 Updated decision-relevant global water risk indicators. *World Resources Institute: Washington, DC, USA*.
537
- 538 Holdridge, L. R. (1947). Determination of world plant formations from simple climatic data. *Science*, 105(2727),
539 367–368. <https://doi.org/10.1126/science.105.2727.367>
540
- 541 Holdridge, L. R. (1967). In *Life zone ecology*. *Tropical Science Center*.
542
- 543 Jackson, N. D., Konar, M., Debaere, P., & Sheffield, J. (2021). Crop-specific exposure to extreme temperature and
544 moisture for the globe for the last half century. *Environ. Res. Lett.*, 20. <https://doi.org/10.1088/1748-9326/abf8e0>
545
- 546 Kamali, B., Abbaspour, K. C., Wehrli, B., & Yang, H. (2019). A Quantitative Analysis of Socio-Economic
547 Determinants Influencing Crop Drought Vulnerability in Sub-Saharan Africa. *Sustainability*, 11(21).
548 <https://doi.org/10.3390/su11216135>
549
- 550 Kuhn, M. (2020). *caret: Classification and Regression Training*. Retrieved from [https://CRAN.R-](https://CRAN.R-project.org/package=caret)
551 [project.org/package=caret](https://CRAN.R-project.org/package=caret)
552
- 553 Kummu, M., Taka, M., & Guillaume, J. H. A. (2018). Gridded global datasets for Gross Domestic Product and
554 Human Development Index over 1990–2015. *Scientific Data*, 5(1), 180004. <https://doi.org/10.1038/sdata.2018.4>
555
- 556 Kummu, M., Heino, M., Taka, M., Varis, O., & Viviroli, D. (2021). Climate change risks pushing one-third of
557 global food production outside the safe climatic space. *One Earth*, 4(5), 720–729.
558 <https://doi.org/10.1016/j.oneear.2021.04.017>
559
- 560 Lehner, B., & Grill, G. (2013). Global river hydrography and network routing: baseline data and new approaches to
561 study the world's large river systems. *Hydrological Processes*, 27(15), 2171–2186. <https://doi.org/10.1002/hyp.9740>
562
- 563 Leng, G., & Hall, J. W. (2020). Predicting spatial and temporal variability in crop yields: an inter-comparison of
564 machine learning, regression and process-based models. *Environmental Research Letters*, 15(4), 044027.
565 <https://doi.org/10.1088/1748-9326/ab7b24>

566

567 Leutner, B., Horning, N., & Schwalb-Willmann, J. (2019). *RStoolbox: Tools for Remote Sensing Data Analysis*.
568 Retrieved from <https://CRAN.R-project.org/package=RStoolbox>

569

570 Lu, C., & Tian, H. (2017). Global nitrogen and phosphorus fertilizer use for agriculture production in the past half
571 century: shifted hot spots and nutrient imbalance. *Earth System Science Data*, 9(1), 181–192.
572 <https://doi.org/10.5194/essd-9-181-2017>

573

574 MacDonald, G. K., Brauman, K. A., Sun, S., Carlson, K. M., Cassidy, E. S., Gerber, J. S., & West, P. C. (2015).
575 Rethinking Agricultural Trade Relationships in an Era of Globalization. *BioScience*, 65(3), 275–289.
576 <https://doi.org/10.1093/biosci/biu225>

577

578 Meyer, H., Reudenbach, C., Wöllauer, S., & Nauss, T. (2019). Importance of spatial predictor variable selection in
579 machine learning applications – Moving from data reproduction to spatial prediction. *Ecological Modelling*, 411,
580 108815. <https://doi.org/10.1016/j.ecolmodel.2019.108815>

581

582 Mueller, N. D., Gerber, J. S., Johnston, M., Ray, D. K., Ramankutty, N., & Foley, J. A. (2012). Closing yield gaps
583 through nutrient and water management. *Nature*, 490(7419), 254–257. <https://doi.org/10.1038/nature11420>

584

585 Müller, C., Elliott, J., Pugh, T. A. M., Ruane, A. C., Ciais, P., Balkovic, J., et al. (2018). Global patterns of crop
586 yield stability under additional nutrient and water inputs. *PLOS ONE*, 13(6), e0198748.
587 <https://doi.org/10.1371/journal.pone.0198748>

588

589 Portmann, F. T., Siebert, S., & Döll, P. (2010). MIRCA2000—Global monthly irrigated and rainfed crop areas
590 around the year 2000: A new high-resolution data set for agricultural and hydrological modeling. *Global*
591 *Biogeochemical Cycles*, 24(1). <https://doi.org/10.1029/2008GB003435>

592

593 R Core Team. (2020). *R: A Language and Environment for Statistical Computing*. Vienna, Austria: R Foundation
594 for Statistical Computing. Retrieved from <https://www.R-project.org/>

595

596 Ray, D. K., Ramankutty, N., Mueller, N. D., West, P. C., & Foley, J. A. (2012). Recent patterns of crop yield growth
597 and stagnation. *Nature Communications*, 3(1), 1293. <https://doi.org/10.1038/ncomms2296>

598

599 Ray, D. K., Gerber, J. S., MacDonald, G. K., & West, P. C. (2015). Climate variation explains a third of global crop
600 yield variability. *Nature Communications*, 6(1), 5989. <https://doi.org/10.1038/ncomms6989>

601

- 602 Ray, D. K., West, P. C., Clark, M., Gerber, J. S., Prishchepov, A. V., & Chatterjee, S. (2019). Climate change has
603 likely already affected global food production. *PLOS ONE*, *14*(5), 1–18.
604 <https://doi.org/10.1371/journal.pone.0217148>
605
- 606 Reidsma, P., Ewert, F., Lansink, A. O., & Leemans, R. (2010). Adaptation to climate change and climate variability
607 in European agriculture: The importance of farm level responses. *European Journal of Agronomy*, *32*(1), 91-102.
608 <https://doi.org/10.1016/j.eja.2009.06.003>
609
- 610 Ricciardi, V., Ramankutty, N., Mehrabi, Z., Jarvis, L., & Chookolingo, B. (2018). How much of the world's food do
611 smallholders produce? *Global Food Security*, *17*, 64–72. <https://doi.org/10.1016/j.gfs.2018.05.002>
612
- 613 RStudio Team. (2019). *RStudio: Integrated Development Environment for R*. Boston, MA: RStudio, Inc. Retrieved
614 from <http://www.rstudio.com/>
615
- 616 Ruane, A. C., Goldberg, R., & Chryssanthacopoulos, J. (2015). Climate forcing datasets for agricultural modeling:
617 Merged products for gap-filling and historical climate series estimation. *Agric. Forest Meteorol.*, *200*, 233–248.
618 <https://doi.org/10.1016/j.agrformet.2014.09.016>
619
- 620 Sarhadi, A., Ausín, M. C., Wiper, M. P., Touma, D., & Diffenbaugh, N. S. (2018). Multidimensional risk in a
621 nonstationary climate: Joint probability of increasingly severe warm and dry conditions. *Science Advances*, *4*(11),
622 eaau3487. <https://doi.org/10.1126/sciadv.aau3487>
623
- 624 Siebert, S., Kummu, M., Porkka, M., Döll, P., Ramankutty, N., & Scanlon, B. R. (2015). A global data set of the
625 extent of irrigated land from 1900 to 2005. *Hydrology and Earth System Sciences*, *19*(3), 1521–1545.
626 <https://doi.org/10.5194/hess-19-1521-2015>
627
- 628 Simelton, E., Fraser, E. D. G., Termansen, M., Forster, P. M., & Dougill, A. J. (2009). Typologies of crop-drought
629 vulnerability: an empirical analysis of the socio-economic factors that influence the sensitivity and resilience to
630 drought of three major food crops in China (1961–2001). *Environmental Science & Policy*, *12*(4), 438–452.
631 <https://doi.org/10.1016/j.envsci.2008.11.005>
632
- 633 Simelton, E., Fraser, E. D. G., Termansen, M., Benton, T. G., Gosling, S. N., South, A., et al. (2012). The
634 socioeconomics of food crop production and climate change vulnerability: a global scale quantitative analysis of
635 how grain crops are sensitive to drought. *Food Security*, *4*(2), 163–179. <https://doi.org/10.1007/s12571-012-0173-4>
636
- 637 Smits, J., & Permanyer, I. (2019). The Subnational Human Development Database. *Scientific Data*, *6*(1), 190038.
638 <https://doi.org/10.1038/sdata.2019.38>

639

640 Tigchelaar, M., Battisti, D. S., Naylor, R. L., & Ray, D. K. (2018). Future warming increases probability of globally
641 synchronized maize production shocks. *Proceedings of the National Academy of Sciences*, *115*(26), 6644–6649.

642 <https://doi.org/10.1073/pnas.1718031115>

643

644 Tilman, D., Balzer, C., Hill, J., & Befort, B. L. (2011). Global food demand and the sustainable intensification of
645 agriculture. *Proceedings of the National Academy of Sciences*, *108*(50), 20260.

646 <https://doi.org/10.1073/pnas.1116437108>

647

648 Troy, T. J., Kipgen, C., & Pal, I. (2015). The impact of climate extremes and irrigation on US crop yields.

649 *Environmental Research Letters*, *10*(5), 054013. <https://doi.org/10.1088/1748-9326/10/5/054013>

650

651 Varis, O., Taka, M., & Kummu, M. (2019). The Planet's Stressed River Basins: Too Much Pressure or Too Little
652 Adaptive Capacity? *Earth's Future*, *7*(10), 1118–1135. <https://doi.org/10.1029/2019EF001239>

653

654 Vogel, E., Donat, M. G., Alexander, L. V., Meinshausen, M., Ray, D. K., Karoly, D., et al. (2019). The effects of
655 climate extremes on global agricultural yields. *Environmental Research Letters*, *14*(5), 054010.

656 <https://doi.org/10.1088/1748-9326/ab154b>

657

658 West, P. C., Gerber, J. S., Engstrom, P. M., Mueller, N. D., Brauman, K. A., Carlson, K. M., et al. (2014). Leverage
659 points for improving global food security and the environment. *Science*, *345*(6194), 325.

660 <https://doi.org/10.1126/science.1246067>

661

662 WGI. (2018). The worldwide governance indicators. Retrieved from Retrieved from Washington D.C.:

663 <http://info.worldbank.org/governance/wgi/#home>

Over Half of the Negative Crop Yield Variability Explained by Anthropogenic Indicators

P. Kinnunen*¹, M. Heino¹, V. Sandström¹, M. Taka¹, D. K. Ray², M. Kummu*¹

¹ Water and Development Research Group, Aalto University, Espoo, Finland

² Institute on the Environment, University of Minnesota, Twin Cities, USA

*Corresponding author: Pekka Kinnunen (pekka.kinnunen@aalto.fi), Matti Kummu (matti.kummu@aalto.fi)

Contents of this file

Figures S1 to S10

Introduction

This supporting information provides additional figures to support the findings of the main text.

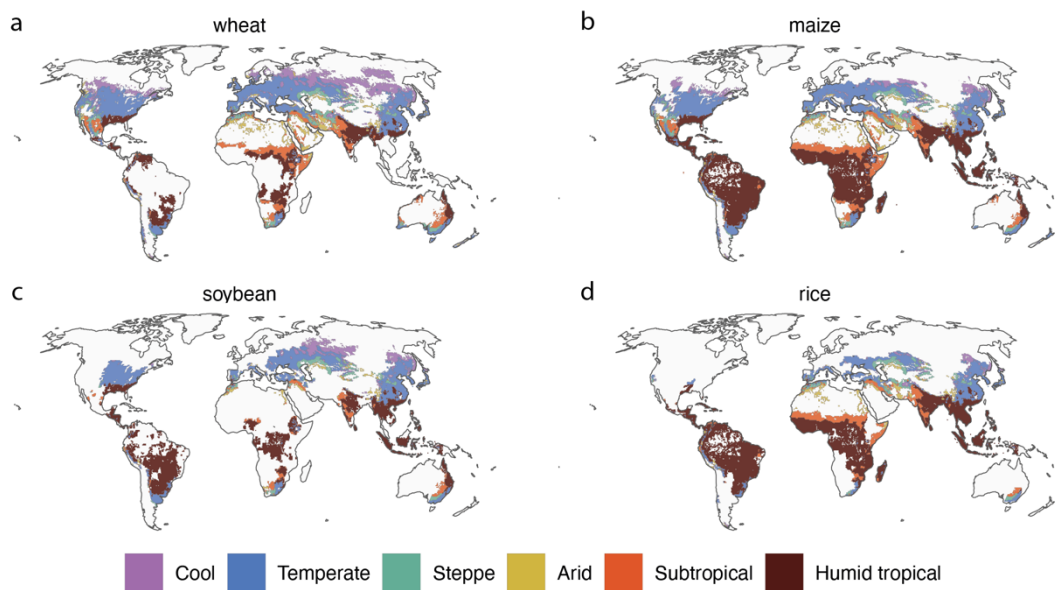


Fig. S1 Holdridge areas intersected with crop growing areas for a. wheat, b. maize, c. soybean and d. rice.

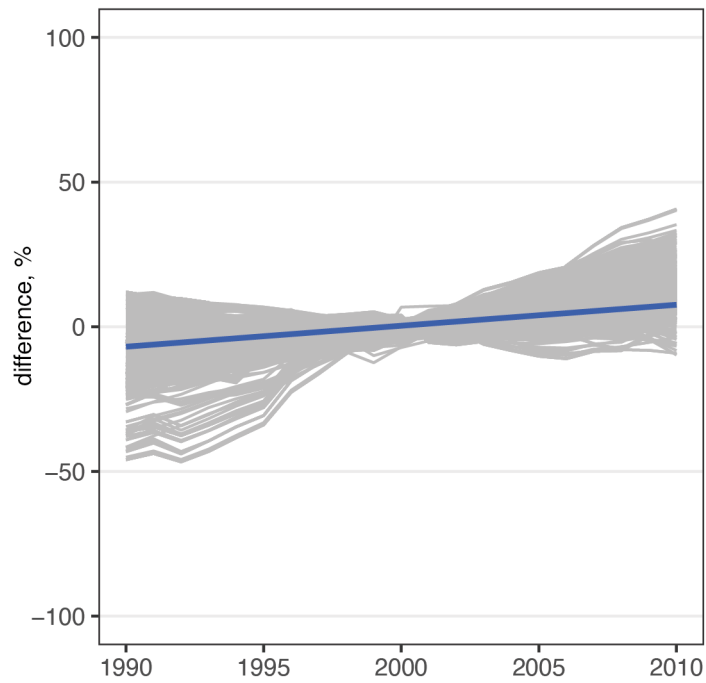


Fig. S2 Difference of subnational Human Development Index (HDI) values (1990-2010) compared to the mean of 1995-2005. We sampled 5000 grid cells from the subnational HDI raster and plotted the timeseries for HDI values for each grid point. Grey lines portray values for the grid cells and blue line depicts linear trend for all the sampled grid cells.

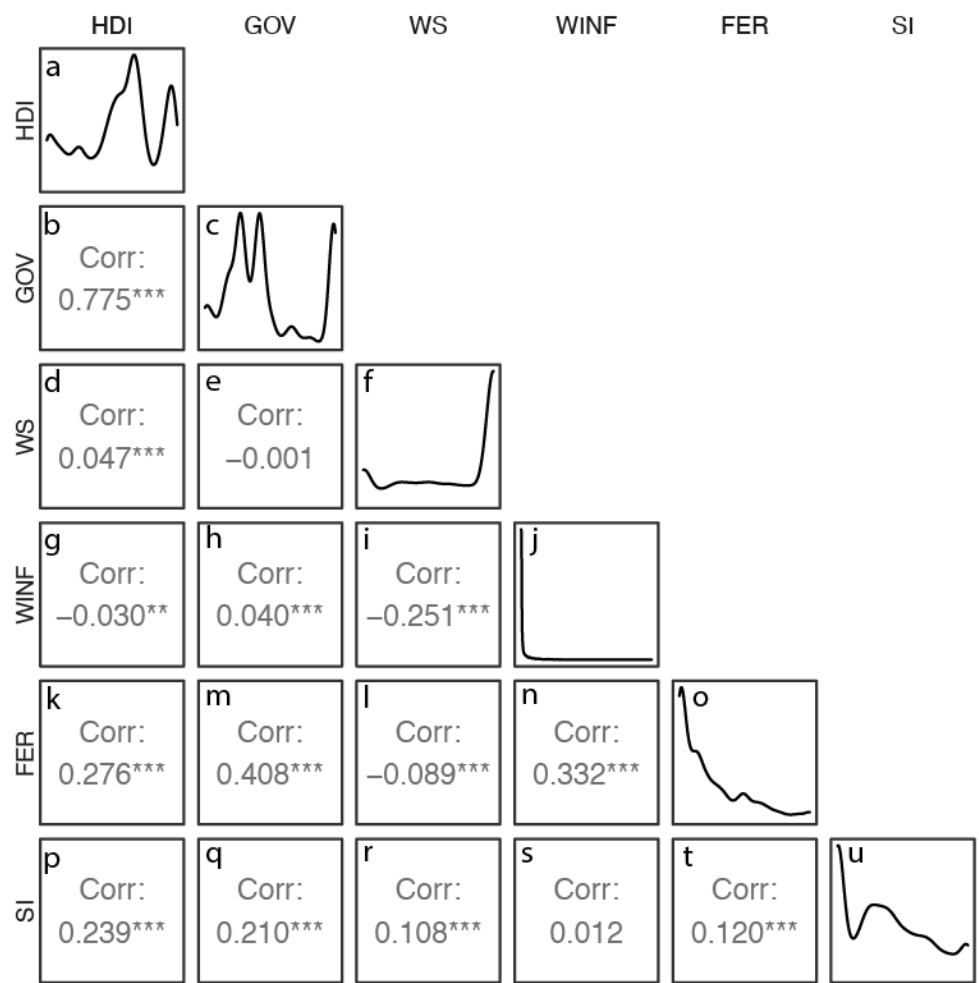


Fig. S3 Distributions (diagonal) and variable correlations for the anthropogenic indicators.

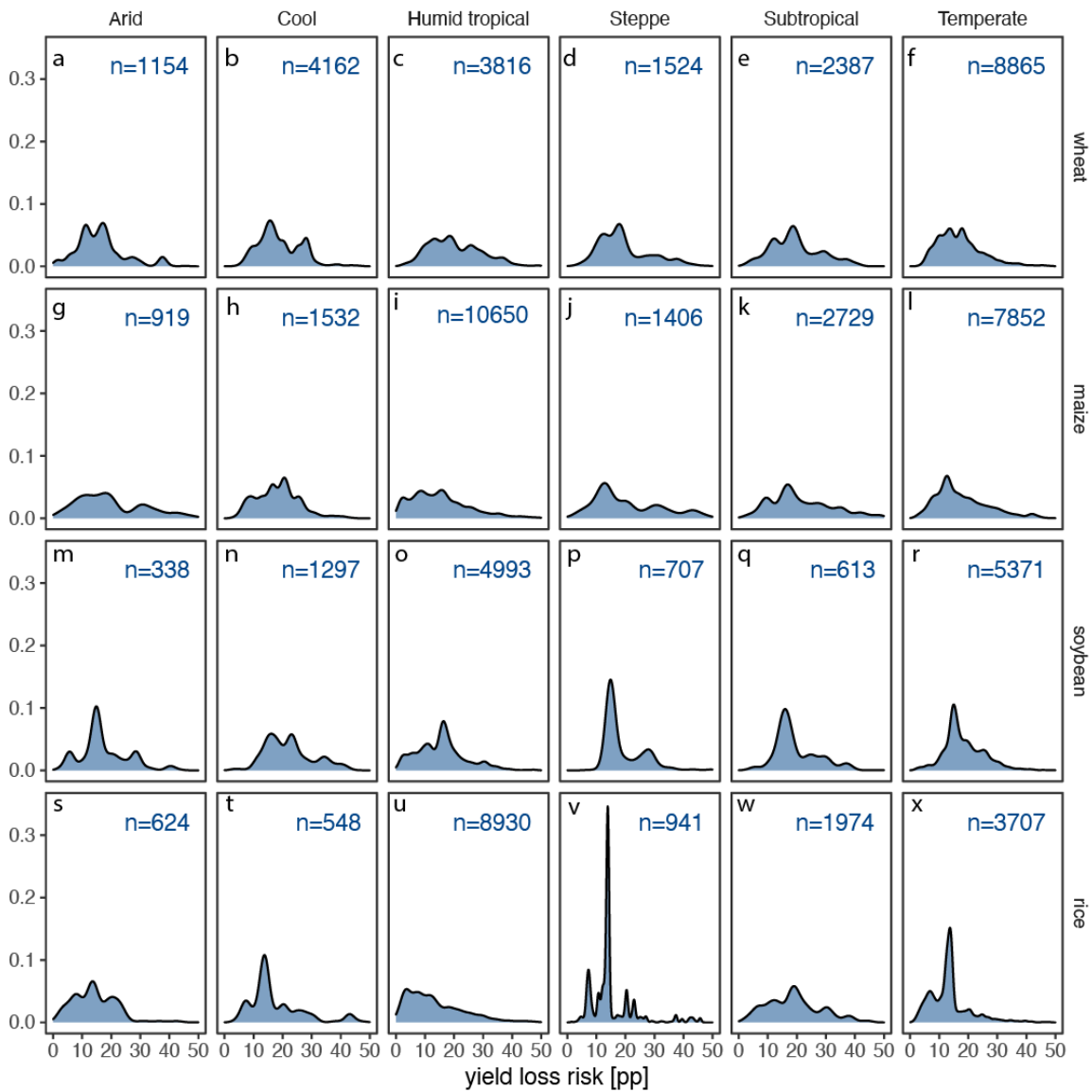


Fig. S4 Distributions and sample sizes (number of cells) used to train the models in the yield loss risk - case. Higher yield loss risk indicates that a grid cell has larger spread in negative yield anomalies (yields lower than running 5-year average) during the study period.

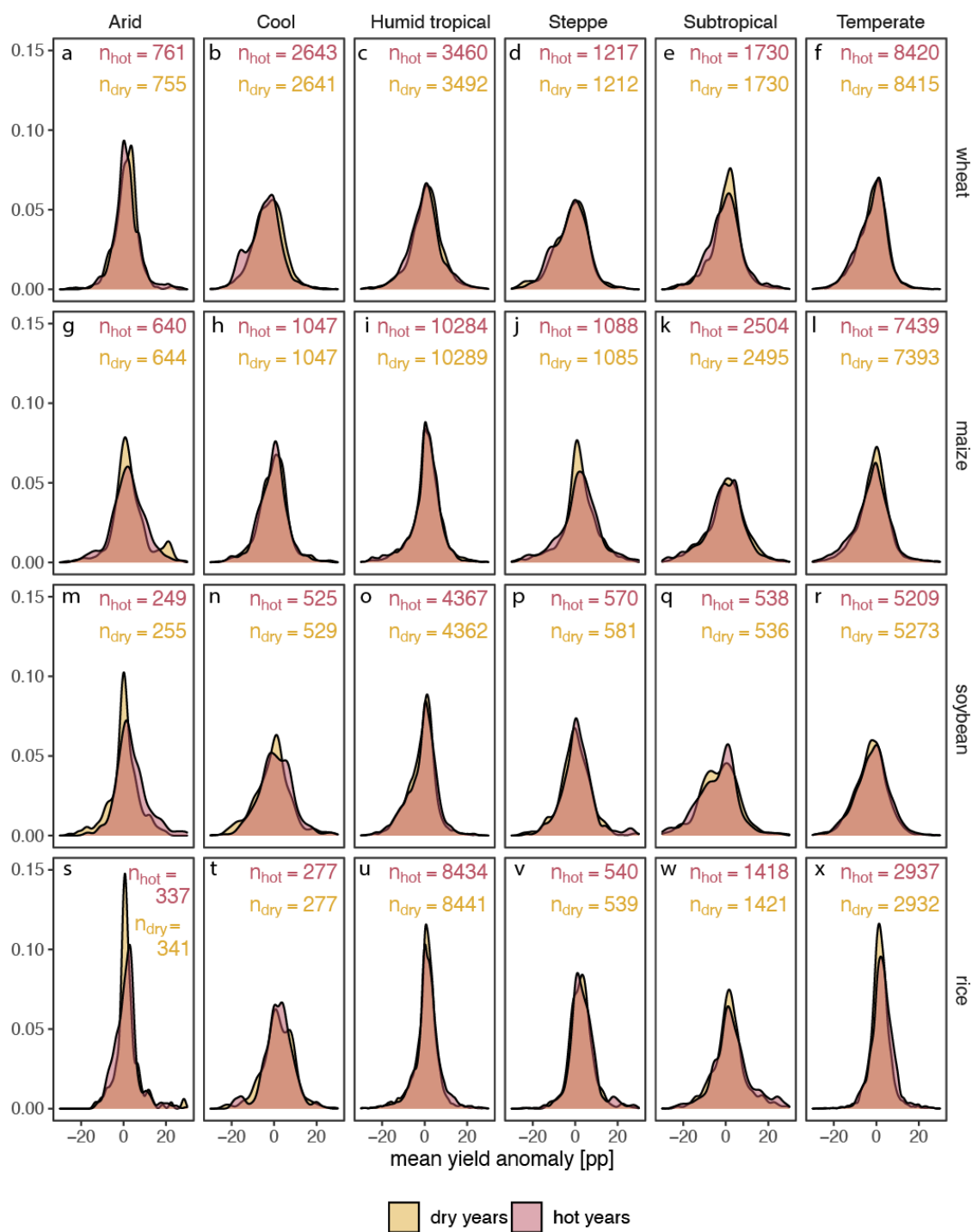


Fig. S5 Distributions and sample sizes (number of cells) used to train the models in the shock factor - cases. Dry years are those when soil moisture deficit is in the >90th percentile is more than 1 standard deviation from the long-term mean (as the number of days). Hot years indicate that the number of days when air temperature is in the 90-100% percentile is more than 1 standard deviation from the long-term mean.

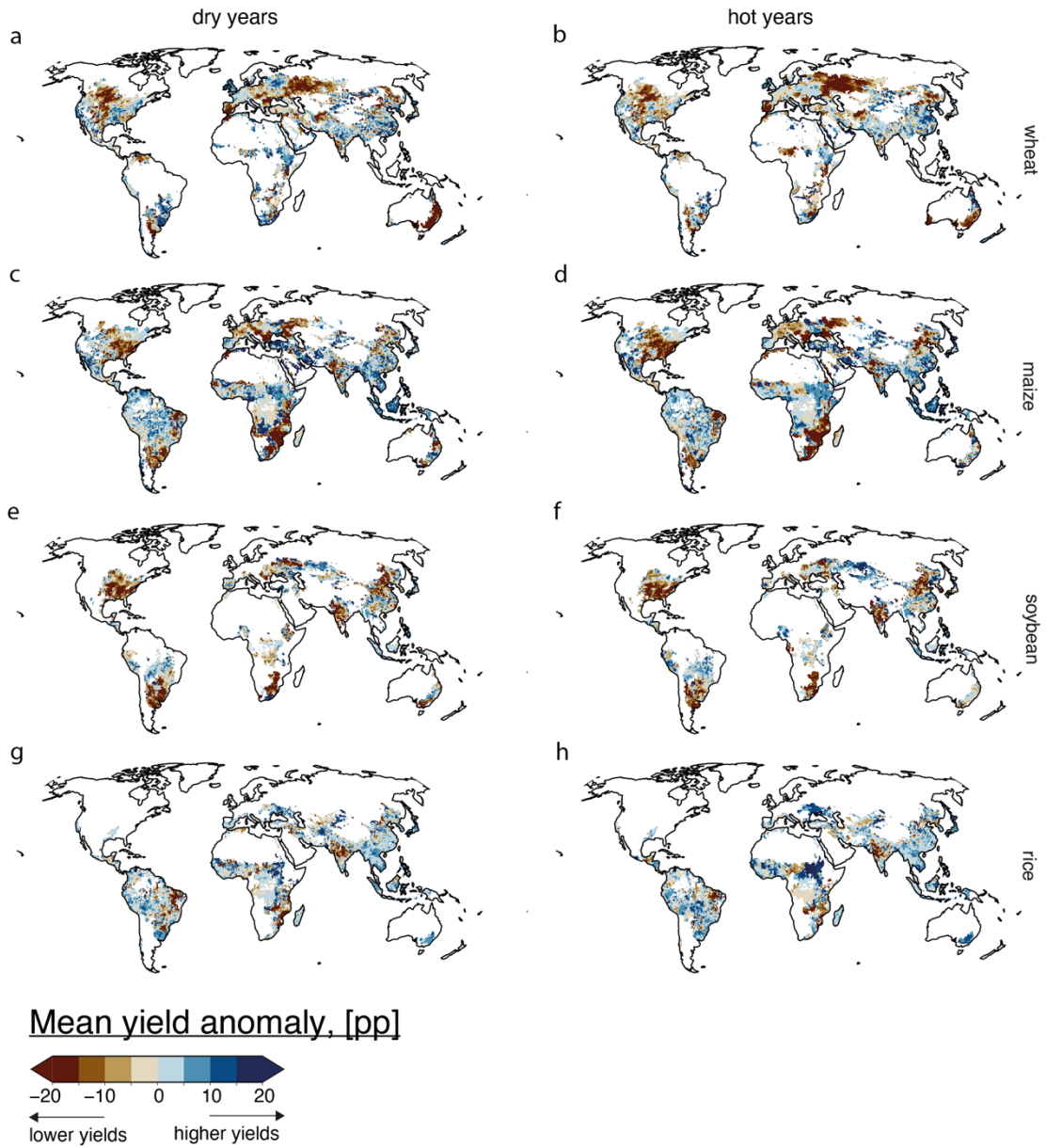


Fig. S6 Mean yield anomalies during shock years. The sign of the yield anomaly indicates whether the mean yields for shock years are higher (positive values; blue) or lower (negative values; brown) than the running 5-year mean yield. Dry years are those when number of days with soil moisture deficit in the >90th percentile is more than 1 standard deviations from the long-term mean. Hot years indicate that the number of days when number of days with air temperature in the >90th percentile is more than 1 standard deviation from the long-term mean.

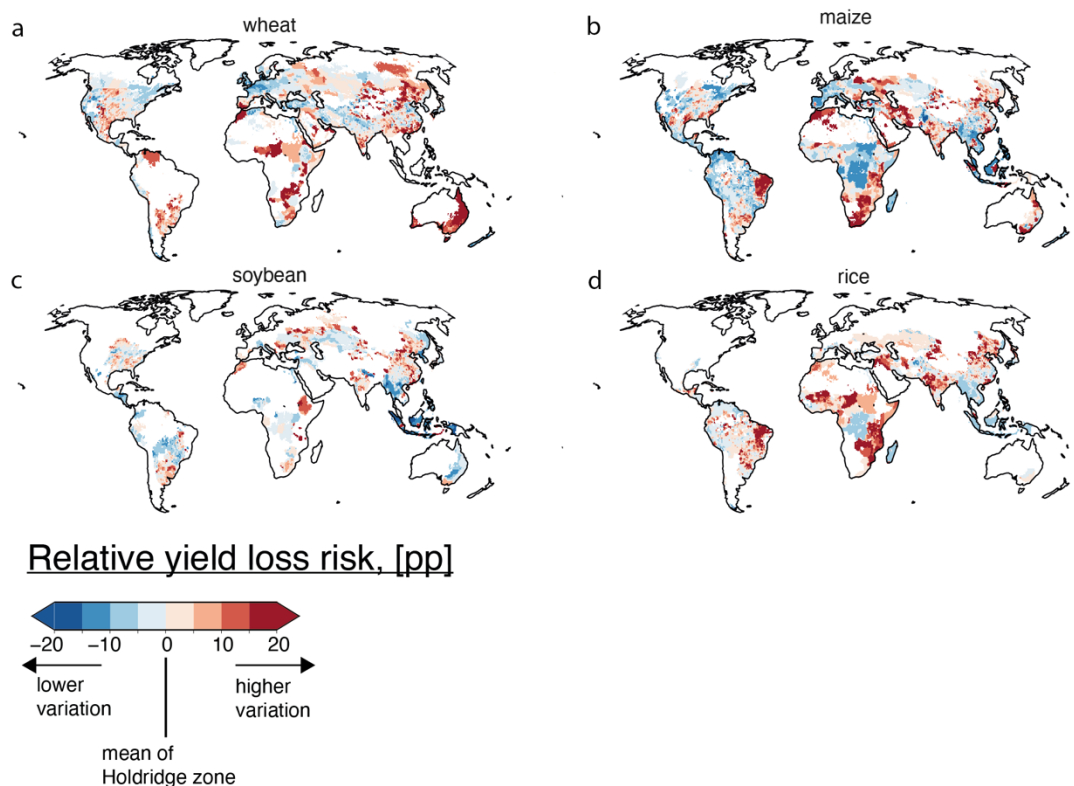


Fig. S7 Difference (as percentage points) between yield loss risk (standard deviation of negative yield anomalies) compared to the mean yield loss risk weighted by mean harvested area for a Holdridge zone for **a. wheat**, **b. maize**, **c. soybean**, and **d. rice**. Increasing yield loss risk (in red) indicates that a grid cell has larger spread in negative yield anomalies (yields lower than running 5-year average) during the study period compared to the mean yield loss risk of the respective Holdridge zone. Decreasing yield loss risk in (blue) indicates smaller variation in negative yield anomalies compared to the weighted mean of the respective Holdridge zone. Values close to zero indicate that the yields align the Holdridge zone's mean yields over 1981-2009, and white areas indicate no production of the crop in question.

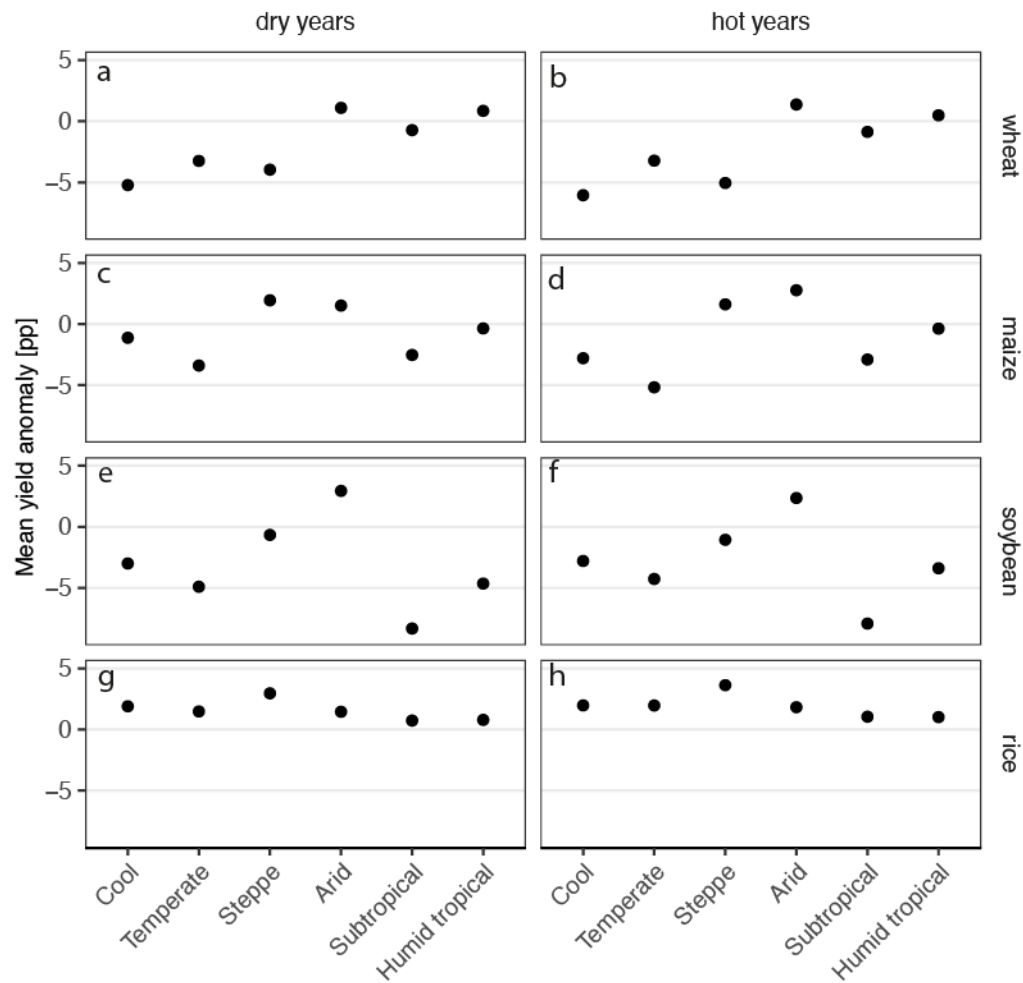


Fig. S9 Mean yield anomalies during temperature ("hot") and soil moisture ("dry") shock years in Holdridge zones. Dry years are those when soil moisture deficit is in the >90th percentile is more than 1 standard deviation from the long-term mean (as the number of days). Hot years indicate that the number of days when air temperature is in the 90-100% percentile is more than 1 standard deviation from the long-term mean.

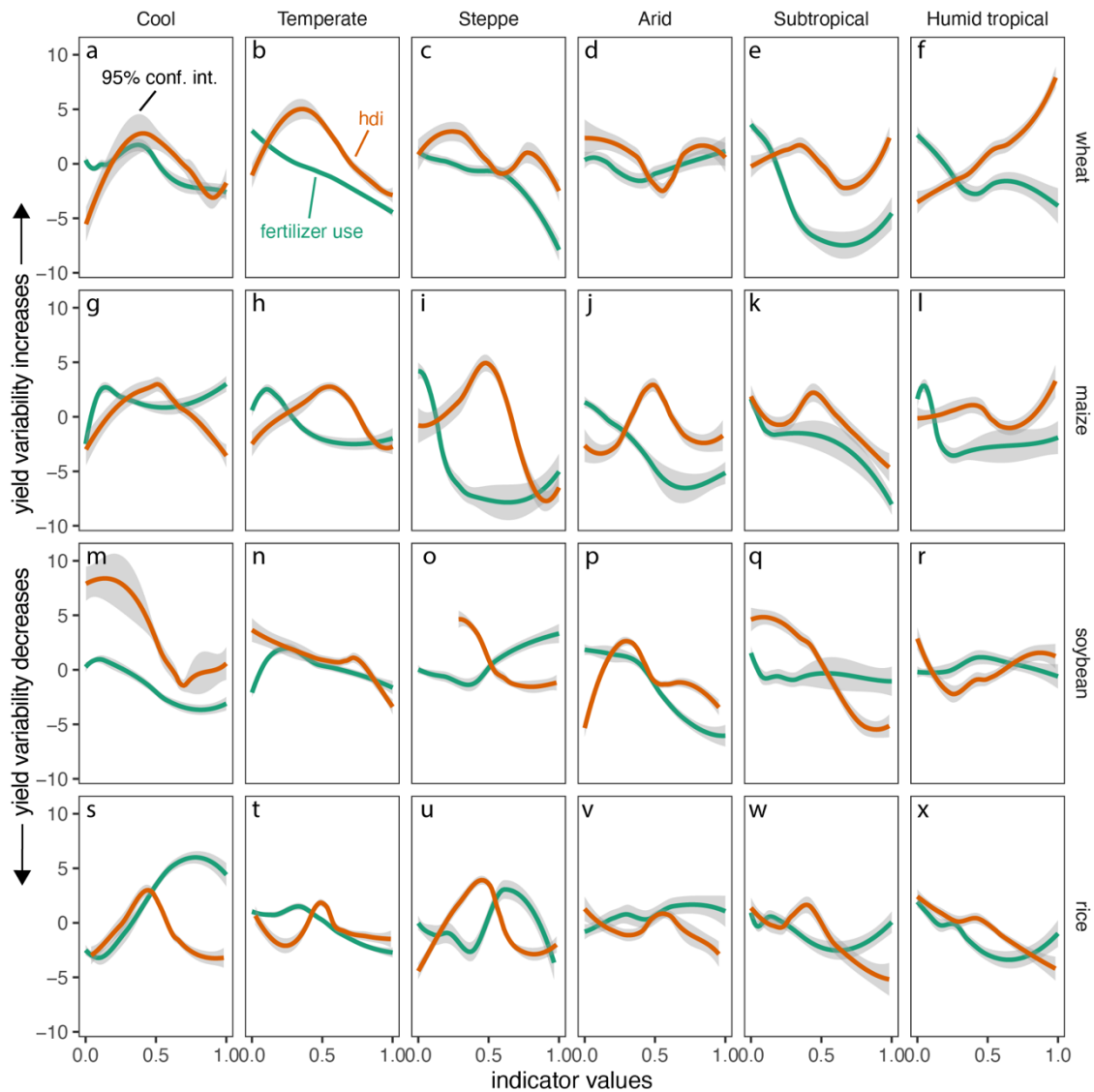


Fig. S10 Main effects for normalized subnational human development index (SHDI) and fertilizer use for assessing the negative crop yield variation at each Holdridge zone from Cool to Humid tropical. The effects are estimated using accumulated local effects -plot (ALE-plot) (Apley & Zhu, 2020) from the 10 models fitted for each crop and Holdridge zone combination aggregated using loess-smoothing. The ALE-plot shows the average marginal effect that the indicator has on the model's outcome variable. The figure shows the magnitude of the effect on yield loss risk (y-axis) with given indicator values (x-axis). The shaded areas indicate 95% confidence intervals.

References

Apley, D. W., & Zhu, J. (2020). Visualizing the effects of predictor variables in black box supervised learning models. *Journal of the Royal Statistical Society: Series B (Statistical Methodology)*, 82(4), 1059–1086. <https://doi.org/10.1111/rssb.12377>